

Linear Precoding Based on Truncated Polynomial Expansion—Part I: Large-Scale Single-Cell Systems

Axel Müller, *Student Member, IEEE*, Abba Kammoun, *Member, IEEE*, Emil Björnson, *Member, IEEE*,
and Mérouane Debbah, *Senior Member, IEEE*

Abstract—Large-scale multi-user multiple-input multiple-output (MIMO) techniques have the potential to bring tremendous improvements for future communication systems. Counter-intuitively, the practical issues of having uncertain channel knowledge, high propagation losses, and implementing optimal non-linear precoding are solved more-or-less automatically by enlarging system dimensions. However, the computational precoding complexity grows with the system dimensions. For example, the close-to-optimal regularized zero-forcing (RZF) precoding is very complicated to implement in practice, since it requires fast inversions of large matrices in every coherence period. Motivated by the high performance of RZF, we propose to replace the matrix inversion by a truncated polynomial expansion (TPE), thereby obtaining the new TPE precoding scheme which is more suitable for real-time hardware implementation. The degree of the matrix polynomial can be adapted to the available hardware resources and enables smooth transition between simple maximum ratio transmission (MRT) and more advanced RZF.

By deriving new random matrix results, we obtain a deterministic expression for the asymptotic signal-to-interference-and-noise ratio (SINR) achieved by TPE precoding in large-scale MIMO systems. Furthermore, we provide a closed-form expression for the polynomial coefficients that maximizes this SINR. To maintain a fixed per-user rate loss as compared to RZF, the polynomial degree does not need to scale with the system, but it should be increased with the quality of the channel knowledge and the signal-to-noise ratio (SNR).

Index Terms—Large-scale MIMO, linear precoding, multi-user systems, polynomial expansion, random matrix theory.

I. INTRODUCTION

The current wireless networks must be greatly densified to meet the exponential growth in data traffic and number of user terminals (UTs) [1]. The conventional densification approach is to decrease the inter-site distance by adding new base stations (BSs) [2]. However, the cells are subject to more interference from neighboring cells as distances shrink, which requires substantial coordination between neighboring BSs or fractional frequency reuse patterns. Furthermore, serving high-mobility UTs by small cells is very cumbersome due to the large overhead caused by rapidly recurring handover.

Large-scale multiple-input multiple-output (MIMO) techniques, also known as massive MIMO techniques, have been

shown to be viable alternatives or complements to small cells [3]–[7]. By deploying large-scale arrays with very many antennas at current macro BSs, an exceptional array gain and spatial precoding resolution can be obtained. This is exploited to achieve higher UT rates and serve more UTs simultaneously. In this paper, we consider the single-cell downlink case where one BS with M antennas serves K single-antenna UTs. As a rule-of-thumb, hundreds of BS antennas may be deployed in the near future to serve tenths of UTs in parallel. If the UTs are selected spatially to have a very small number of common scatterers, the user channels naturally decorrelate as M grows large [8], [9] and space-division multiple access (SDMA) techniques become robust to channel uncertainty [3].

One might imagine that by taking M and K large, it becomes terribly difficult to optimize the system throughput. The beauty of large-scale multi-user MIMO is that this is not the case: simple linear precoding is asymptotically optimal when $M \gg K$ [3] and random matrix theory can provide simple deterministic approximations of the stochastic achievable rates [5], [10]–[14]. These so-called *deterministic equivalents* are tight as M grows large due to channel hardening, but are usually also very accurate at small values of M and K .

Although linear precoding is computationally more efficient than its non-linear alternatives, the complexity of most linear precoding schemes is still intractable in the large- (M, K) regime since the number of arithmetic operations is proportional to K^2M . For example, both the optimal precoding parametrization in [15] and the near-optimal *regularized zero-forcing* (RZF) precoding [16] require an inversion of the Gram matrix of the joint channel of all users—this matrix operation has cubic complexity. A notable exception is the matched filter, also known as *maximum ratio transmission* (MRT) [17], which has only square complexity. Unfortunately, this precoding scheme might require an order of magnitude more BS antennas to perform as well as RZF [5]. Treating the precoding complexity problem is the main focus of this paper.

Similar complexity issues appear in multi-user detection, where the minimum mean squared error (MMSE) detector involves matrix inversions [18]. This uplink problem has received considerable attention in the last two decades; see [18]–[21] and references therein. In particular, different reduced-rank filtering approaches have been proposed, often based on the concept of *truncated polynomial expansion* (TPE). Simply speaking, the idea is to approximate the matrix inverse by a matrix polynomial with J terms, where J needs not to scale with the system dimensions to maintain a certain approximation accuracy [19]. TPE-based detectors admit simple and

A. Kammoun, A. Müller, E. Björnson, and M. Debbah are with the Alcatel-Lucent Chair on Flexible Radio, SUPELEC, Gif-sur-Yvette, France (e-mail: {abba.kammoun, axel.mueller, emil.bjornson, merouane.debbah}@supelec.fr). E. Björnson is also with the Department of Signal Processing, ACCESS Linnaeus Centre, KTH Royal Institute of Technology, Stockholm, Sweden.

E. Björnson is funded by the International Postdoc Grant 2012-228 from The Swedish Research Council. This research has been supported by the ERC Starting Grant 305123 MORE (Advanced Mathematical Tools for Complex Network Engineering).

efficient multistage/pipelined hardware implementation [18], which stands in contrast to the complicated implementation of matrix inversion. A key requirement to achieve good detection performance at small J is to find good coefficients for the polynomial. This has been a major research challenge because the optimal coefficients are expensive to compute [18]. Alternatives based on appropriate scaling [20] and asymptotic analysis [21] have been proposed. A similar TPE-based approach was used in [22] for the purpose of low-complexity channel estimation in large-scale MIMO systems.

In this paper, we propose a new family of low-complexity linear precoding schemes for the single-cell multi-user downlink. We exploit TPE to enable a balancing of precoding complexity and system throughput. A main analytic contribution is derivation of deterministic equivalents for the achievable user rates for any order J of TPE precoding. These expressions are tight when M and K grow large with a fixed ratio, but also provide close approximations at small parameter values. The deterministic equivalents allow for optimization of the polynomial coefficients; we derive the coefficients that maximize the throughput. We note that this approach for precoding design is very new. The only other work is [23] by Zarei *et al.*, of which we just became aware at the time of submission. Unlike our work, the precoding in [23] is conceived to minimize the sum-MSE of all users. Although our approach originates from the same idea as in [23], the design method proposed herein is more efficient since it considers the optimization of the throughput. This metric is usually more pertinent than the sum-MSE. Additionally, our work is more comprehensive in that we consider a channel model which takes into account the transmit correlation at the base station.

Our novel TPE precoding scheme enables a smooth transition in performance between MRT ($J = 1$) and RZF ($J = \min(M, K)$), where the majority of the gap is bridged for small values of J . We show that J is independent of the system dimensions M and K , but must increase with the signal-to-noise ratio (SNR) and channel state information (CSI) quality to maintain a fixed per-user rate gap to RZF. We stress that the polynomial structure provides a green radio approach to precoding, since it enables energy-efficient multistage hardware implementation as compared to the complicated/inefficient signal processing required to compute conventional RZF. Furthermore, the hardware complexity can be easily tailored to the deployment scenario or even changed dynamically by increasing and reducing J in high and low SNR situations, respectively.

A. Notation

Boldface (lower case) is used for column vectors, \mathbf{x} , and (upper case) for matrices, \mathbf{X} . Let \mathbf{X}^T , \mathbf{X}^H , and \mathbf{X}^* denote the transpose, conjugate transpose, and conjugate of \mathbf{X} , respectively, while $\text{tr}(\mathbf{X})$ is the matrix trace function. The Frobenius norm is denoted $\|\cdot\|$ and the spectral norm is denoted $\|\cdot\|_2$. A circularly symmetric complex Gaussian random vector \mathbf{x} is denoted $\mathbf{x} \sim \mathcal{CN}(\bar{\mathbf{x}}, \mathbf{Q})$, where $\bar{\mathbf{x}}$ is the mean and \mathbf{Q} is the covariance matrix. The set of all complex numbers is denoted by \mathbb{C} , with $\mathbb{C}^{N \times 1}$ and $\mathbb{C}^{N \times M}$ being the generalizations to

vectors and matrices, respectively. The $M \times M$ identity matrix is written as \mathbf{I}_M and the zero vector of length M is denoted $\mathbf{0}_{M \times 1}$. For an infinitely differentiable monovariate function $f(t)$, the ℓ th derivative at $t = t_0$ (i.e., $d^\ell/dt^\ell f(t)|_{t=t_0}$) is denoted by $f^{(\ell)}(t_0)$ and more concisely $f^{(\ell)}$, when $t = 0$. An analog definition is considered in the bivariate case; in particular $f^{(l,m)}(t_0, u_0)$ refers to the ℓ th and m th derivative with respect to t and u at t_0 and u_0 , respectively (i.e., $\partial^\ell/\partial t^\ell \partial^m/\partial u^m f(t, u)|_{t=t_0, u=u_0}$). If $t_0 = u_0 = 0$ we abbreviate again as $f^{(l,m)} = f^{(l,m)}(0, 0)$. Furthermore, we use the big- O and small- o notation in their usual sense; that is, $\alpha_M = \mathcal{O}(\beta_M)$ serves a flexible abbreviation for $|\alpha_M| \leq C\beta_M$, where C is a generic constant, and $\alpha_M = o(\beta_M)$ is shorthand for $\alpha_M = \varepsilon_M \beta_M$ with $\varepsilon_M \rightarrow 0$, as M goes to infinity.

II. SYSTEM MODEL

This section defines the single-cell system with flat-fading channels, linear precoding, and channel estimation errors.

A. Transmission Model

We consider a single-cell downlink system in which a BS, equipped with M antennas, serves K single-antenna UTs. The received complex baseband signal $y_k \in \mathbb{C}$ at the k th UT is given by

$$y_k = \mathbf{h}_k^H \mathbf{x} + n_k, \quad k = 1, \dots, K \quad (1)$$

where $\mathbf{x} \in \mathbb{C}^{M \times 1}$ is the transmit signal and $\mathbf{h}_k \in \mathbb{C}^{M \times 1}$ represents the random channel vector between the BS and the k th UT. The additive circularly-symmetric complex Gaussian noise at the k th UT is denoted by $n_k \sim \mathcal{CN}(0, \sigma^2)$ for $k = 1, \dots, K$, where σ^2 is the receiver noise variance.

The small-scale channel fading is modeled as follows.

Assumption A-1. The channel vector \mathbf{h}_k is modeled as

$$\mathbf{h}_k = \Phi^{\frac{1}{2}} \mathbf{z}_k \quad (2)$$

where the channel covariance matrix $\Phi \in \mathbb{C}^{M \times M}$ has bounded spectral norm $\|\Phi\|_2$, as $M \rightarrow \infty$, and $\mathbf{z}_k \sim \mathcal{CN}(\mathbf{0}_{M \times 1}, \mathbf{I}_M)$. The channel vector has a fixed realization for a coherence period and then takes a new independent realization. This model is known as Rayleigh block-fading.

Note that all UTs have the same covariance matrix which facilitates simpler analysis (cf. [11], [13], [16]) and thereby set the focus on our precoding contribution. This means, in practice, that the scattering environment is very rich in the area where the UTs reside. The covariance matrix can either be a scaled identity matrix or describe array-specific properties (e.g., radiation pattern) and general propagation properties of the coverage area. Extensions to fully user-specific covariance matrices can be obtained by following the approach in [12] or the approach in our companion multi-cell paper [24].

Assumption A-2. The BS employs Gaussian codebooks and linear precoding, where $\mathbf{g}_k \in \mathbb{C}^{M \times 1}$ denotes the precoding vector and $s_k \sim \mathcal{CN}(0, 1)$ is the data symbol of the k th UT.

Based on this assumption, the transmit signal in (1) is

$$\mathbf{x} = \sum_{n=1}^K \mathbf{g}_n s_n = \mathbf{G}\mathbf{s}. \quad (3)$$

The matrix notation is obtained by letting $\mathbf{G} = [\mathbf{g}_1 \dots \mathbf{g}_K] \in \mathbb{C}^{M \times K}$ be the precoding matrix and $\mathbf{s} = [s_1 \dots s_K]^T \sim \mathcal{CN}(\mathbf{0}_{K \times 1}, \mathbf{I}_K)$ be the vector containing all UT data symbols.

Consequently, the received signal (1) can be expressed as

$$y_k = \mathbf{h}_k^H \mathbf{g}_k s_k + \sum_{n=1, n \neq k}^K \mathbf{h}_k^H \mathbf{g}_n s_n + n_k. \quad (4)$$

Let $\mathbf{G}_k \in \mathbb{C}^{M \times (K-1)}$ be the matrix \mathbf{G} with column \mathbf{g}_k removed. Then the SINR at the k th UT becomes

$$\text{SINR}_k = \frac{\mathbf{h}_k^H \mathbf{g}_k \mathbf{g}_k^H \mathbf{h}_k}{\mathbf{h}_k^H \mathbf{G}_k \mathbf{G}_k^H \mathbf{h}_k + \sigma^2}. \quad (5)$$

By assuming that each UT has perfect instantaneous CSI, the achievable data rates at the UTs are

$$r_k = \log_2(1 + \text{SINR}_k), \quad k = 1, \dots, K.$$

B. Model of Imperfect Channel Information at Transmitter

Since we typically have $M \geq K$ in practice, we assume that we either have a time-division duplex (TDD) protocol where the BS acquires channel knowledge from uplink pilot signaling [5] or a frequency-division duplex (FDD) protocol where temporal correlation is exploited as in [25]. In both cases, the transmitter generally has imperfect knowledge of the instantaneous channel realizations and we model this by the generic Gauss-Markov formulation from [12], [26], [27]:

Assumption A-3. *The transmitter has an imperfect channel estimate*

$$\hat{\mathbf{h}}_k = \Phi^{\frac{1}{2}} \left(\sqrt{1-\tau^2} \mathbf{z}_k + \tau \mathbf{v}_k \right) = \sqrt{1-\tau^2} \mathbf{h}_k + \tau \mathbf{n}_k \quad (6)$$

for each UT, $k = 1, \dots, K$, where \mathbf{h}_k is the true channel, $\mathbf{v}_k \sim \mathcal{CN}(\mathbf{0}_{M \times 1}, \mathbf{I}_M)$, and $\mathbf{n}_k = \Phi^{\frac{1}{2}} \mathbf{v}_k \sim \mathcal{CN}(\mathbf{0}_{M \times 1}, \Phi)$ models the independent error. The scalar parameter $\tau \in [0, 1]$ indicates the quality of the instantaneous CSI, where $\tau = 0$ corresponds to perfect instantaneous CSI and $\tau = 1$ corresponds to having only statistical channel knowledge.

The parameter τ depends on factors such as time/power spent on pilot-based channel estimation and user mobility. Note that we assume for simplicity that the BS has the same quality of channel knowledge for all UTs.

Based on the model in (6), the matrix

$$\hat{\mathbf{H}} = [\hat{\mathbf{h}}_1 \dots \hat{\mathbf{h}}_K] \in \mathbb{C}^{M \times K} \quad (7)$$

denotes the joint imperfect knowledge of all user channels.

III. LINEAR PRECODING

Many heuristic linear precoding schemes have been proposed in the literature, mainly because finding the optimal precoding (in terms of weighted sum rate or other criteria) is very computational demanding and thus unsuitable for fading systems [28]. Among the heuristic schemes we distinguish

RZF precoding [16], which is also known as the transmit Wiener filter [29], signal-to-leakage-and-noise ratio maximizing beamforming [30], generalized eigenvalue-based beamformer [31], and virtual SINR maximizing beamforming [32]. The reason that RZF precoding has been proposed by different authors (under different names) is, most likely, that it can provide close-to-optimal performance in many scenarios. It also outperforms classical MRT and zero-forcing beamforming (ZFBF) by combining the respective benefits of these schemes [28]. Therefore, RZF is deemed the natural starting point for this paper.

Next, we provide a brief review of RZF and prior performance results in large-scale MIMO systems. These results serve as a starting point for Section III-B, where we propose an alternative precoding scheme with a computational/hardware complexity more suited for large systems.

A. Review on RZF Precoding in Large-Scale MIMO Systems

Suppose we have a total transmit power constraint

$$\text{tr}(\mathbf{G}\mathbf{G}^H) = P. \quad (8)$$

We stress that the total power P is fixed, while we let the number of antennas, M , and number of UTs, K , grow large.

Similar to [12], we define the RZF precoding matrix as

$$\begin{aligned} \mathbf{G}_{\text{RZF}} &= \frac{\beta}{\sqrt{K}} \hat{\mathbf{H}} \left(\frac{1}{K} \hat{\mathbf{H}}^H \hat{\mathbf{H}} + \xi \mathbf{I}_K \right)^{-1} \mathbf{P}^{\frac{1}{2}} \\ &= \beta \left(\frac{1}{K} \hat{\mathbf{H}} \hat{\mathbf{H}}^H + \xi \mathbf{I}_M \right)^{-1} \frac{\hat{\mathbf{H}}}{\sqrt{K}} \mathbf{P}^{\frac{1}{2}} \end{aligned} \quad (9)$$

where the power normalization parameter β is set such that \mathbf{G}_{RZF} satisfies the power constraint in (8) and \mathbf{P} is a fixed diagonal matrix whose diagonal elements are power allocation weights for each user. We assume that \mathbf{P} satisfies:

Assumption A-4. *The diagonal values p_k , $k = 1, \dots, K$ in $\mathbf{P} = \text{diag}(p_1, \dots, p_K)$ are positive and of order $\mathcal{O}(\frac{1}{K})$.*

The scalar regularization coefficient ξ can be selected in different ways, depending on the noise variance, channel uncertainty at the transmitter, and system dimensions [12], [16]. In [12], the performance of each UT under RZF precoding is studied in the large- (M, K) regime. This means that M and K tend to infinity at the same speed, which can be formalized as follows.

Assumption A-5. *In the large- (M, K) regime, M and K tend to infinity such that*

$$0 < \liminf \frac{K}{M} \leq \limsup \frac{K}{M} < +\infty.$$

The user performance is characterized by SINR_k in (5). Although the SINR is a random quantity that depends on the instantaneous values of the random users channels in \mathbf{H} and the instantaneous estimate $\hat{\mathbf{H}}$, it can be approximated using deterministic quantities in the large- (M, K) regime [10]–[13]. These are quantities that only depend on the statistics of the channels and are often referred to as *deterministic equivalents*, since they are almost surely (a.s.) tight in the asymptotic limit. This channel hardening property is essentially due to the law of

large numbers. Deterministic equivalents were first proposed by Hachem *et al.* in [10], who have also shown their ability to capture important system performance indicators. When the deterministic equivalents are applied at finite M and K , they are referred to as *large-scale approximations*.

In the sequel, by deterministic equivalent of a sequence of random variables X_n we mean a deterministic sequence \bar{X}_n which approximates X_n such that

$$X_n - \bar{X}_n \xrightarrow[n \rightarrow +\infty]{\text{a.s.}} 0. \quad (10)$$

As an example, we recall the following result from [10], which provides some widely known results on deterministic equivalents. Note that we have chosen to work with a slightly different definition of the deterministic equivalents than in [10], since this better fits the analysis of our proposed precoding scheme.

Theorem 1 (Adapted from [10]). *Consider the resolvent matrix $\mathbf{Q}(t) = (\frac{t}{K} \mathbf{H} \mathbf{H}^H + \mathbf{I}_M)^{-1}$ where the columns of \mathbf{H} are distributed according to Assumption A-1. Then, the equation*

$$\delta(t) = \frac{1}{K} \text{tr} \left(\Phi \left(\mathbf{I}_M + \frac{t \Phi}{1 + t \delta(t)} \right)^{-1} \right)$$

admits a unique solution $\delta(t) > 0$ for every $t > 0$.

Let $\mathbf{T}(t) = (\mathbf{I}_M + \frac{t \Phi}{1 + t \delta(t)})^{-1}$ and let \mathbf{U} be any matrix with bounded spectral norm. Under Assumption A-5 and for $t > 0$, we have

$$\frac{1}{K} \text{tr}(\mathbf{U} \mathbf{Q}(t)) - \frac{1}{K} \text{tr}(\mathbf{U} \mathbf{T}(t)) \xrightarrow[M, K \rightarrow +\infty]{\text{a.s.}} 0. \quad (11)$$

The statement in (11) shows that $\frac{1}{K} \text{tr}(\mathbf{U} \mathbf{T}(t))$ is a deterministic equivalent to the random quantity $\frac{1}{K} \text{tr}(\mathbf{U} \mathbf{Q}(t))$.

In this paper, the deterministic equivalents are essential to determine the limit to which the SINRs tend in the large- (M, K) regime. For RZF precoding, as in (9), this limit is given by the following theorem.

Theorem 2 (Adapted from Corollary 1 in [12]). *Let $\rho = \frac{P}{\sigma^2}$ and consider the notation $\mathbf{T} = \mathbf{T}(\frac{1}{\xi})$ and $\delta = \delta(\frac{1}{\xi})$. Define the deterministic scalar quantities*

$$\gamma = \frac{1}{K} \text{tr}(\mathbf{T} \Phi \mathbf{T} \Phi)$$

and

$$\theta = \frac{(1 - \tau^2) \frac{p_k}{P/K} \delta^2 ((\delta + \xi)^2 - \gamma)}{\gamma (\xi^2 - \tau^2 (\xi^2 - (\xi + \delta)^2)) + \frac{1}{K} \text{tr}(\Phi \mathbf{T}^2) \frac{(\xi + \delta)^2}{\rho}}. \quad (12)$$

Then, the SINRs with RZF precoding satisfies

$$\text{SINR}_k - \theta \xrightarrow[M, K \rightarrow +\infty]{\text{a.s.}} 0, \quad k = 1, \dots, K.$$

Note that all UTs obtain the same asymptotic value of the SINR, since the UTs have homogeneous channel statistics. Theorem 2 holds for any regularization coefficient ξ , but the parameter can also be selected to maximize the limiting value θ of the SINRs. This is achieved by the following theorem.

Theorem 3 (Adapted from Proposition 2 in [12]). *Under the assumption of a uniform power allocation, $p_k = \frac{P}{K}$, the large-scale approximated SINR in (12) under RZF precoding is*

maximized by the regularization parameter ξ^ , given as the positive solution to the fixed-point equation*

$$\xi^* = \frac{1}{\rho (1 - \tau^2) (1 + \nu(\xi^*)) + \frac{1}{(\xi^*)^2} \tau^2 \nu(\xi^*) (\xi + \delta)^2} \frac{1 + \nu(\xi^*) + \tau^2 \rho \frac{\gamma}{\frac{1}{K} \text{tr}(\Phi \mathbf{T}^3)}}{1}$$

where $\nu(\xi)$ is given by

$$\nu(\xi) = \frac{\xi \frac{1}{K} \text{tr}(\Phi \mathbf{T}^3)}{\gamma \frac{1}{K} \text{tr}(\Phi \mathbf{T}^2)} \left(\frac{\gamma}{\frac{1}{K} \text{tr}(\Phi \mathbf{T}^2)} - \frac{\frac{1}{K} \text{tr}(\Phi^2 \mathbf{T}^3)}{\frac{1}{K} \text{tr}(\Phi \mathbf{T}^3)} \right).$$

The RZF precoding matrix in (9) is a function of the instantaneous CSI at the transmitter. Although the SINRs converges to the deterministic equivalents given in Theorem 2, in the large- (M, K) regime, the precoding matrix remains a random quantity that is typically recalculated on a millisecond basis (i.e., at the same pace as the channel knowledge is updated). This is a major practical issue, because the matrix inversion operation in RZF precoding is very computationally demanding in large systems [33]; the number of operations scale as $\mathcal{O}(K^2 M)$ and the known inversion algorithms are complicated to implement in hardware (see Section IV for details). The matrix inversion is the key to interference suppression in RZF precoding, thus there is need to develop less complicated precoding schemes that still can suppress interference efficiently.

B. Truncated Polynomial Expansion Precoding

Motivated by the inherent complexity issues of RZF precoding, we now develop a new linear precoding class that much easier to implement in large systems. The precoding is based on rewriting the matrix inversion by a polynomial expansion, which is then truncated. The following lemma provides a major motivation behind the use of polynomial expansions.

Lemma 4. *For any positive definite Hermitian matrix \mathbf{X} ,*

$$\mathbf{X}^{-1} = \kappa (\mathbf{I} - (\mathbf{I} - \kappa \mathbf{X}))^{-1} = \kappa \sum_{\ell=0}^{\infty} (\mathbf{I} - \kappa \mathbf{X})^{\ell} \quad (13)$$

where the second equality holds if the parameter κ is selected such that $0 < \kappa < \frac{2}{\max_n \lambda_n(\mathbf{X})}$.

Proof: The inverse of an Hermitian matrix can be computed by inverting each eigenvalue, while keeping the eigenvectors fixed. This lemma follows by applying the standard Taylor series expansion $(1-x)^{-1} = \sum_{\ell=0}^{\infty} x^{\ell}$, for any $|x| < 1$, on each eigenvalue of the Hermitian matrix $(\mathbf{I} - \kappa \mathbf{X})$. The condition on x corresponds to requiring that the spectral norm $\|\mathbf{I} - \kappa \mathbf{X}\|_2$ is bounded by unity, which holds for $\kappa < \frac{2}{\max_n \lambda_n(\mathbf{X})}$. See [20] for an in-depth analysis of such properties of polynomial expansions. ■

This lemma shows that the inverse of any Hermitian matrix can be expressed as a matrix polynomial. More importantly, the low-order terms are the most influential ones, since the eigenvalues of $(\mathbf{I} - \kappa \mathbf{X})^{\ell}$ converge geometrically to zero as ℓ grows large. This is due to each eigenvalue λ of $(\mathbf{I} - \kappa \mathbf{X})$ having an absolute value smaller than unity, $|\lambda| < 1$, and thus λ^{ℓ} goes geometrically to zero as $\ell \rightarrow \infty$. As such, it makes sense to consider a TPE of the matrix inverse using

only the first J terms. This corresponds to approximating the inversion of each eigenvalue by a Taylor polynomial with J terms, hence the approximation accuracy per matrix element is independent of M and K ; that is, J needs not change with the system dimensions.

TPE has been successfully applied for low-complexity multi-user detection in [18]–[21] and channel estimation in [22]. Next, we exploit the TPE technique to approximate RZF precoding by a matrix polynomial. Starting from \mathbf{G}_{RZF} in (9), we note that

$$\beta \left(\frac{1}{K} \hat{\mathbf{H}} \hat{\mathbf{H}}^H + \xi \mathbf{I}_M \right)^{-1} \frac{\hat{\mathbf{H}}}{\sqrt{K}} \mathbf{P}^{\frac{1}{2}} \quad (14)$$

$$= \beta \kappa \sum_{\ell=0}^{\infty} \left(\mathbf{I}_M - \kappa \left(\frac{1}{K} \hat{\mathbf{H}} \hat{\mathbf{H}}^H + \xi \mathbf{I}_M \right) \right)^{\ell} \frac{\hat{\mathbf{H}}}{\sqrt{K}} \mathbf{P}^{\frac{1}{2}} \quad (15)$$

$$\approx \beta \kappa \sum_{\ell=0}^{J-1} \left(\mathbf{I}_M - \kappa \left(\frac{1}{K} \hat{\mathbf{H}} \hat{\mathbf{H}}^H + \xi \mathbf{I}_M \right) \right)^{\ell} \frac{\hat{\mathbf{H}}}{\sqrt{K}} \mathbf{P}^{\frac{1}{2}} \quad (16)$$

$$= \sum_{\ell=0}^{J-1} \left(\beta \kappa \sum_{n=\ell}^{J-1} \binom{n}{\ell} (1-\kappa\xi)^{n-\ell} (-\kappa)^{\ell} \right) \times \left(\frac{1}{K} \hat{\mathbf{H}} \hat{\mathbf{H}}^H \right)^{\ell} \frac{\hat{\mathbf{H}}}{\sqrt{K}} \mathbf{P}^{\frac{1}{2}} \quad (17)$$

where (15) follows directly from Lemma 4 (for an appropriate selection of κ), (16) is achieved by truncating the polynomial (only keeping the first J terms), and (17) follows from applying the binomial theorem and gathering the terms for each exponent. Inspecting (17), we have a precoding matrix with the structure

$$\mathbf{G}_{\text{TPE}} = \sum_{\ell=0}^{J-1} w_{\ell} \left(\frac{1}{K} \hat{\mathbf{H}} \hat{\mathbf{H}}^H \right)^{\ell} \frac{\hat{\mathbf{H}}}{\sqrt{K}} \mathbf{P}^{\frac{1}{2}} \quad (18)$$

where w_0, \dots, w_{J-1} are scalar coefficients. Although the bracketed term in (17) provides a potential expression for w_{ℓ} , we stress that these are generally not the optimal coefficients when $J < \infty$. Also, these coefficients are not satisfying the power constraint in (8) since the coefficients are not adapted to the truncation. Hence, we treat w_0, \dots, w_{J-1} as design parameters that should be selected to maximize the performance; for example, by maximizing the limiting value of the SINRs, as was done in Theorem 3 for RZF precoding. We note especially that the value of κ in (17) does not need to be explicitly known in order to choose, optimize and implement the coefficients. We only need for κ to exist, which is always the case under Assumption A-2. Besides the simplified structure, the proposed precoding matrix \mathbf{G}_{TPE} possesses a higher number of degrees of freedom (represented by the J scalars w_{ℓ}) than the RZF precoding (which has only the regularization coefficient ξ).

The precoding in (18) is coined *TPE precoding* and actually defines a whole class of precoding matrices for different J . For $J = 1$ we obtain $\mathbf{G} = \frac{w_0}{\sqrt{K}} \hat{\mathbf{H}} \mathbf{P}^{\frac{1}{2}}$, which equals MRT. Furthermore, RZF precoding can be obtained by choosing $J = \min(M, K)$ and coefficients based on the characteristic polynomial of $(\frac{1}{K} \hat{\mathbf{H}} \hat{\mathbf{H}}^H + \xi \mathbf{I}_M)^{-1}$ (directly from Cayley-Hamilton theorem). We refer to J as the *TPE order* and note that the corresponding polynomial degree is $J-1$. Clearly,

proper selection of J enables a smooth transition between the traditional low-complexity MRT and the high-complexity RZF precoding. Based on the discussion that followed Lemma 4, we assume that the parameter J is a finite constant that does not grow with M and K .

IV. COMPLEXITY ANALYSIS

The complexities of RZF and TPE precoding are described and compared in this section. There are many aspects to take into account. The number of arithmetic operations (additions, multiplications, and divisions) is a classic metric, but also very crude in the sense that it ignores implementation aspects. The ability to parallelize operations and to customize algorithm-specific circuits has a fundamental impact on the computational delays and energy consumption in practical systems.

A. Total Arithmetic Operations for RZF and TPE Precoding

In order to compare the number of arithmetic operations needed for conventional RZF precoding and the proposed TPE precoding, it is important consider how often each operation is repeated. There are two time scales: operations that take place once per coherence period (i.e., once per channel realization) and operations that take place every time the channel is used for downlink transmission. To differentiate between these time scales, we let T_{data} denote the number of downlink data symbols transmitted per coherence period. Recall from (3) that the transmit signal is $\mathbf{G}\mathbf{s}$, where the precoding matrix $\mathbf{G} \in \mathbb{C}^{M \times K}$ changes once per coherence period and the data symbol $\mathbf{s} \in \mathbb{C}^{K \times 1}$ is different at each channel use.

The RZF precoding matrix in (9) is computed once per coherence period. There are two equivalent expressions in (9), where the difference is that the matrix inversion is either of dimension $K \times K$ or $M \times M$. Since $K \leq M$ in most cases of practical interest, we consider the first precoding expression: $\frac{1}{\sqrt{K}} \hat{\mathbf{H}} \left(\frac{1}{K} \hat{\mathbf{H}}^H \hat{\mathbf{H}} + \xi \mathbf{I}_K \right)^{-1} \mathbf{P}^{\frac{1}{2}}$. Assuming that $\frac{1}{\sqrt{K}} \hat{\mathbf{H}}$ and $\mathbf{P}^{\frac{1}{2}}$ are available in advance, we need to 1) compute the matrix-matrix multiplication $(\frac{1}{\sqrt{K}} \hat{\mathbf{H}}^H)(\frac{1}{\sqrt{K}} \hat{\mathbf{H}})$; 2) add the diagonal matrix $\xi \mathbf{I}_K$ to the result; 3) compute $\frac{1}{\sqrt{K}} \hat{\mathbf{H}} \left(\frac{1}{K} \hat{\mathbf{H}}^H \hat{\mathbf{H}} + \xi \mathbf{I}_K \right)^{-1}$ as M linear systems of equations (each having K equations and unknowns); and 4) multiply the result with the diagonal matrix $\mathbf{P}^{\frac{1}{2}}$. These are all standard matrix operations, thus the numbers of arithmetic operations are well-known [34]: $\frac{1}{2}K(K+1)(2M-1)$, K , $\frac{K^3}{3} + 2K^2M$, and MK operations, respectively. The linear systems of equations are solved by computing a Cholesky factorization of $\frac{1}{K} \hat{\mathbf{H}}^H \hat{\mathbf{H}} + \xi \mathbf{I}_K$ and then exploit back-substitution. There are other ways to achieve the same result, but this is among the most efficient algorithms for matrices of practical sizes.¹ When \mathbf{G}_{RZF} has been computed, the matrix-vector multiplication $\mathbf{G}_{\text{RZF}}\mathbf{s}$ requires $M(2K-1)$

¹Matrix multiplication and matrix inversion can be implemented using the Strassen's algorithm in [35] and the improved Coppersmith-Winograd algorithm in [36]. These are divide-and-conquer algorithms that exploit that 2×2 matrices can be multiplied efficiently and thereby reduce the asymptotic complexity of multiplying/inverting $K \times K$ matrices to $\mathcal{O}(K^{2.8074})$ and $\mathcal{O}(K^{2.373})$, respectively. Unfortunately, the overhead in these algorithms is heavy and thus K needs to be at the order of several thousands to achieve a lower complexity than the Cholesky approach considered in Section IV.

operations per channel use of data transmission. In summary, RZF precoding has a total number of arithmetic operations per coherence period of

$$C_{\text{RZF}} = 3K^2M + 2KM + \frac{K^3}{3} - \frac{K^2}{2} + \frac{K}{2} + T_{\text{data}}(2KM - M). \quad (19)$$

Next, we consider TPE precoding. Let the transmit signal with TPE precoding at channel use t be denoted $\mathbf{x}^{(t)}$ and observe that it can be expressed as

$$\mathbf{x}^{(t)} = \mathbf{G}_{\text{TPE}} \mathbf{s}^{(t)} = \sum_{\ell=0}^{J-1} w_{\ell} \tilde{\mathbf{x}}_{\ell}^{(t)} \quad (20)$$

where $\mathbf{s}^{(t)}$ is the vector of data symbols at channel use t and

$$\tilde{\mathbf{x}}_{\ell}^{(t)} = \begin{cases} \frac{\hat{\mathbf{H}}}{\sqrt{K}} (\mathbf{P}^{\frac{1}{2}} \mathbf{s}^{(t)}), & \ell = 0, \\ \frac{\hat{\mathbf{H}}}{\sqrt{K}} (\frac{\hat{\mathbf{H}}^H}{\sqrt{K}} \tilde{\mathbf{x}}_{\ell-1}^{(t)}), & 1 \leq \ell \leq J-1. \end{cases} \quad (21)$$

This reveals that there is an iterative way of computing the J terms in TPE precoding. The benefit of this approach is that it only involves matrix-vector multiplications. Similar to above, we conclude that the case $\ell = 0$ uses $K + M(2K-1)$ operations and each case $\ell \geq 1$ uses $M(2K-1) + K(2M-1)$ operations. Finally, the multiplication with w_{ℓ} requires M operations for each ℓ . In summary, TPE precoding has a total number of arithmetic operations per coherence period of

$$C_{\text{TPE}} = T_{\text{data}}((4J-2)MK - (J-2)K). \quad (22)$$

When comparing RZF and TPE precoding, we note that the complexity of precomputing the RZF precoding matrix is very large, but it is only done once per coherence period. The corresponding matrix \mathbf{G}_{TPE} for TPE precoding is never computed separately, but only indirectly as $\mathbf{G}_{\text{TPE}} \mathbf{s}$ for each data symbol \mathbf{s} . Intuitively, precomputation is beneficial when the coherence block is long (compared to M and K) and the sequential computation of TPE precoding is beneficial when the system dimensions M and K are large (compared to the coherence block). This is seen from the asymptotic complexity scaling which are $\mathcal{O}(K^2M)$ for RZF precoding and $\mathcal{O}(KM)$ for TPE precoding; thus, the asymptotic difference is huge. The breaking point where TPE precoding outperforms RZF (in terms of number of operations) is easily computed:

$$C_{\text{RZF}} > C_{\text{TPE}} \Rightarrow T_{\text{data}} < \frac{3K^2M + 2KM + \frac{K^3}{3} - \frac{K^2}{2} + \frac{K}{2}}{4(J-1)MK + M - (J-2)K}. \quad (23)$$

One should not forget the overhead signaling required to obtain CSI at the UTs, which makes the number of channel uses T_{data} available for data symbols reduce with K . For example, suppose $T_{\text{coherence}}$ is the total coherence block and that we use a TDD protocol, where η_{DL} is the fraction used for downlink transmission and μK channel uses (for some $\mu \geq 1$) are consumed by downlink pilot signals that provide the UTs with sufficient CSI. We then have $T_{\text{data}} = \eta_{\text{DL}} T_{\text{coherence}} - \mu K$. Using this expression, the number of arithmetic operations are illustrated numerically in Fig. 1 for $\eta_{\text{DL}} = \frac{1}{2}$, $T_{\text{coherence}} =$

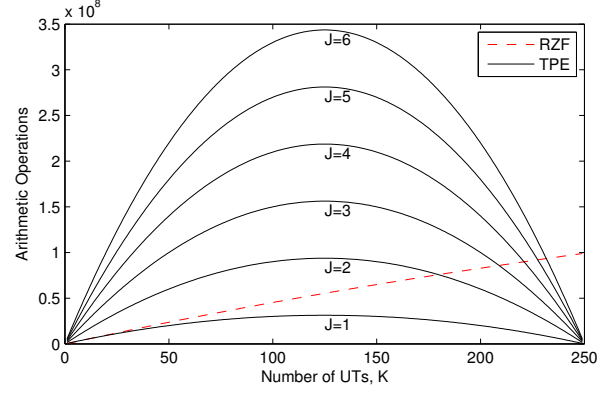


Fig. 1. Total number of arithmetic operations of RZF precoding and TPE precoding (with different J) for $T = 1000$ channel uses and $M = 500$.

1000, and $\mu = 2$.² This figure shows that TPE precoding uses fewer operations than RZF precoding when there are many UTs, while RZF is competitive for smaller number of UTs.

B. Implementation Complexity of RZF and TPE Precoding

In practice, the number of arithmetic operations is not the main issue, but the implementation costs in terms of hardware complexity, time delays, and energy consumption. The analysis in the previous subsection showed that we can only expect minor improvements in the number of arithmetic operations from TPE precoding. The main advantage of TPE precoding is that it enables multistage hardware implementation where the computations are parallelized over multiple processing cores (e.g., application-specific integrated circuits (ASICs)) and pipelined [20]. This structure is illustrated in Fig. 2 where the transmitted signal $\mathbf{x}^{(t)}$ is prepared in parallel with both precoding and succeeding transmit signals. Each processing core performs a simple matrix-vector multiplication which each requires only approximately $T_{\text{data}}(2MK)$ arithmetic operations per coherence period, which are only additions and multiplications. This is relatively easy to implement using ASICs, which are known to be very energy-efficient and have low production cost. Consequently, we can select the TPE order J as large as needed to obtain a certain precoding accuracy and only pay the price of adding a few extra circuits of the same type.

In comparison, the computation of RZF precoding involves many divisions (which typically are less efficient and accurate than additions and multiplications) and is not easily parallelized. Hence, the C_{RZF} arithmetic operations per coherence period are handled by a single processing core, which needs a higher clock-frequency and energy consumption than the TPE precoding implementation. In addition, the precomputation of the RZF precoding matrix might cause non-negligible delays that forces T_{data} to be smaller than for TPE precoding; for example, [33] describes a hardware implementation from [38] where it takes 0.15 ms to compute RZF precoding for $K = 15$, and the number of active UTs can be much larger than

²These parameter values correspond to symmetric downlink/uplink transmission, 2 downlink pilot symbols per UT (at different frequencies), a coherence bandwidth of 200 kHz, and a coherence time of 5 ms. These are similar to the values in the LTE standard [37, Chapter 10].

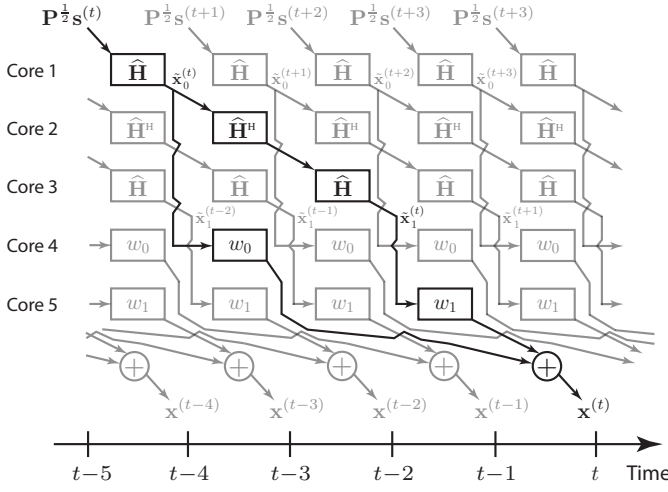


Fig. 2. Illustration of a simple pipelined implementation of the proposed TPE precoding with $J = 2$, which removes the delays caused by precomputing the precoding matrix. Each block performs a simple matrix-vector multiplication, which enables highly efficient hardware implementation and J can be increased by simply adding additional cores.

this in large-scale MIMO systems. TPE precoding does not cause such delays because there are no precomputations—the arithmetic operations are spread over the coherence period.

In practice this means, that only the curve pertaining to $J = 1$ in Fig. 1 is relevant for comparisons of implementation complexity between TPE and RZF; if one is prepared to add as many multiple processing cores as necessary.

V. ANALYSIS AND OPTIMIZATION OF TPE PRECODING

In this section, we consider the large- (M, K) regime, defined in Assumption A-5. We show that SINR_k , for $k = 1, \dots, K$, under TPE precoding converges to a limit, a deterministic equivalent, that depends only on the coefficients w_ℓ , the respective attributed power p_k , and the channel statistics.

Recall the SINR expression in (5) and observe that $\mathbf{g}_k = \mathbf{G}\mathbf{e}_k$ and $\mathbf{h}_k^H \mathbf{G}_k \mathbf{G}_k^H \mathbf{h}_k = \mathbf{h}_k^H \mathbf{G} \mathbf{G}^H \mathbf{h}_k - \mathbf{h}_k^H \mathbf{g}_k \mathbf{g}_k^H \mathbf{h}_k$, where \mathbf{e}_k is the k th column of the identity matrix \mathbf{I}_K . By substituting the TPE precoding expression (18) into (5), it is easy to show that the SINR writes as

$$\text{SINR}_k = \frac{\mathbf{w}^H \mathbf{A}_k \mathbf{w}}{\mathbf{w}^H \mathbf{B}_k \mathbf{w} + \sigma^2} \quad (24)$$

where $\mathbf{w} = [w_0 \dots w_{J-1}]^T$ and the (ℓ, m) th elements of the matrices $\mathbf{A}_k, \mathbf{B}_k \in \mathbb{C}^{J \times J}$ are

$$[\mathbf{A}_k]_{\ell, m} = \frac{p_k}{K} \mathbf{h}_k^H \left(\frac{1}{K} \hat{\mathbf{H}} \hat{\mathbf{H}}^H \right)^\ell \hat{\mathbf{h}}_k \hat{\mathbf{h}}_k^H \left(\frac{1}{K} \hat{\mathbf{H}} \hat{\mathbf{H}}^H \right)^m \mathbf{h}_k \quad (25)$$

$$[\mathbf{B}_k]_{\ell, m} = \frac{1}{K} \mathbf{h}_k^H \left(\frac{1}{K} \hat{\mathbf{H}} \hat{\mathbf{H}}^H \right)^\ell \hat{\mathbf{H}} \mathbf{P} \hat{\mathbf{H}} \left(\frac{1}{K} \hat{\mathbf{H}} \hat{\mathbf{H}}^H \right)^m \mathbf{h}_k - [\mathbf{A}_k]_{\ell, m} \quad (26)$$

for $\ell = 0, \dots, J-1$ and $m = 0, \dots, J-1$.³

Since the random matrices \mathbf{A}_k and \mathbf{B}_k are of finite dimensions, it suffices to determine a deterministic equivalent for each of their elements. To achieve this, we express them using

³The entries of matrices are numbered from 0, for notational convenience.

the resolvent matrix of $\hat{\mathbf{H}}$. This can be done by introducing the following random functionals in t and u :

$$X_{k, M}(t, u) = \frac{1}{K^2} \mathbf{h}_k^H \left(\frac{t}{K} \hat{\mathbf{H}} \hat{\mathbf{H}}^H + \mathbf{I}_M \right)^{-1} \hat{\mathbf{h}}_k \hat{\mathbf{h}}_k^H \left(\frac{u}{K} \hat{\mathbf{H}} \hat{\mathbf{H}}^H + \mathbf{I}_M \right)^{-1} \mathbf{h}_k \quad (27)$$

$$Z_{k, M}(t, u) = \frac{1}{K} \mathbf{h}_k^H \left(\frac{t}{K} \hat{\mathbf{H}} \hat{\mathbf{H}}^H + \mathbf{I} \right)^{-1} \hat{\mathbf{H}} \mathbf{P} \hat{\mathbf{H}} \left(\frac{u}{K} \hat{\mathbf{H}} \hat{\mathbf{H}}^H + \mathbf{I}_K \right)^{-1} \mathbf{h}_k. \quad (28)$$

By taking derivatives of $X_{k, M}(t, u)$ and $Z_{k, M}(t, u)$, we obtain

$$X_{k, M}^{(\ell, m)} = \frac{(-1)^{\ell+m} \ell! m!}{K^2} \mathbf{h}_k^H \left(\frac{\hat{\mathbf{H}} \hat{\mathbf{H}}^H}{K} \right)^\ell \hat{\mathbf{h}}_k \hat{\mathbf{h}}_k^H \left(\frac{\hat{\mathbf{H}} \hat{\mathbf{H}}^H}{K} \right)^m \mathbf{h}_k \quad (29)$$

$$Z_{k, M}^{(\ell, m)} = \frac{(-1)^{\ell+m} \ell! m!}{K} \mathbf{h}_k^H \left(\frac{\hat{\mathbf{H}} \hat{\mathbf{H}}^H}{K} \right)^\ell \hat{\mathbf{H}} \mathbf{P} \hat{\mathbf{H}} \left(\frac{\hat{\mathbf{H}} \hat{\mathbf{H}}^H}{K} \right)^m \mathbf{h}_k. \quad (30)$$

Substituting (29)–(30) into (25)–(26), we obtain the alternative expressions

$$[\mathbf{A}_k]_{\ell, m} = \frac{K p_k (-1)^{\ell+m}}{\ell! m!} X_{k, M}^{(\ell, m)}$$

$$[\mathbf{B}_k]_{\ell, m} = \frac{(-1)^{\ell+m}}{\ell! m!} (K p_k X_{k, M}^{(\ell, m)} + Z_{k, M}^{(\ell, m)}).$$

It, thus, suffices to study the asymptotic convergence of the bivariate functions $X_{k, M}(t, u)$ and $Z_{k, M}(t, u)$. This is achieved by the following new theorem and its corollary:

Theorem 5. Consider a channel matrix $\hat{\mathbf{H}}$ whose columns are distributed according to Assumption A-3. Under the asymptotic regime described in Assumption A-5, we have

$$X_{k, M}(t, u) - \bar{X}_M(t, u) \xrightarrow[M, K \rightarrow +\infty]{\text{a.s.}} 0$$

and

$$K p_k X_{k, M}(t, u) + Z_{k, M}(t, u) - \text{tr}(\mathbf{P}) \bar{b}_M(t, u) \xrightarrow[M, K \rightarrow +\infty]{\text{a.s.}} 0$$

where

$$\bar{X}_M(t, u) = \frac{(1 - \tau^2) \delta(t) \delta(u)}{(1 + t \delta(t))(1 + u \delta(u))}$$

$$\bar{b}_M(t, u) = \left(\tau^2 + \frac{(1 - \tau)^2}{(1 + u \delta(u))(1 + t \delta(t))} \right) \beta_M(t, u)$$

and $\beta_M(t, u)$ is given by

$$\beta_M(t, u) = \frac{\frac{1}{K} \text{tr}(\Phi \mathbf{T}(u) \Phi \mathbf{T}(t))}{(1 + t \delta(t))(1 + u \delta(u)) - \frac{t u}{K} \text{tr}(\Phi \mathbf{T}(u) \Phi \mathbf{T}(t))}. \quad (31)$$

Proof: See Appendix B. ■

Corollary 6. Assume that Assumptions A-1 and A-5 hold true. Then, we have

$$X_{k, M}^{(\ell, m)} - \bar{X}_M^{(\ell, m)} \xrightarrow[M, K \rightarrow +\infty]{\text{a.s.}} 0$$

and

$$\left(p_k X_{k, M}^{(\ell, m)} + Z_{k, M}^{(\ell, m)} \right) - \text{tr}(\mathbf{P}) \bar{b}_M^{(\ell, m)} \xrightarrow[M, K \rightarrow +\infty]{\text{a.s.}} 0.$$

Proof: See Appendix D. ■

Corollary 6 shows that the entries of \mathbf{A}_k and \mathbf{B}_k , which depend on the derivatives of $X_{k,M}(t, u)$ and $Z_{k,M}(t, u)$, can be approximated in the asymptotic regime by $\mathbf{T}^{(\ell)}$ and $\delta^{(\ell)}$, which are the derivatives of $\mathbf{T}(t)$ and $\delta(t)$ at $t = 0$. Such derivatives can be computed numerically using the iterative algorithm of [21].

It remains to compute the aforementioned derivatives. To this end, we denote $f(t) = \frac{1}{1+t\delta(t)}$ and $\mathcal{T}(t) = f(t)\mathbf{T}(t)$ and by $f^{(\ell)}$ and $\mathcal{T}^{(\ell)}$ their derivatives. Rewriting (31) as

$$\beta_M(t, u) \left(1 - \frac{tu}{K} \text{tr}(\Phi \mathcal{T}(u) \Phi \mathcal{T}(t)) \right) = \frac{1}{K} \text{tr}(\Phi \mathcal{T}(u) \Phi \mathcal{T}(t))$$

and using the Leibniz derivation rule, we obtain for any integers ℓ and m greater than 1, the expression

$$\begin{aligned} \beta_M^{(\ell, m)} &= \frac{1}{K} \text{tr}(\Phi \mathcal{T}^{(\ell)} \Phi \mathcal{T}^{(m)}) \\ &+ \sum_{k=1}^{\ell-1} \sum_{n=1}^{m-1} kn \binom{\ell}{k} \binom{m}{n} \beta_M^{(k-1, n-1)} \frac{1}{K} \text{tr}(\Phi \mathcal{T}^{(\ell-k)} \Phi \mathcal{T}^{(m-n)}). \end{aligned}$$

An iterative algorithm for the computation of $\beta_M^{(\ell, m)}$ is given by Algorithm 1 in Appendix E. With these derivation results on hand, we are now in the position to determine the expressions for the derivatives of the quantities of interest, namely $\bar{X}_{k,m}(t, u)$ and $\bar{b}_M(t, u)$. Using again the Leibniz derivation rule, we obtain

$$\begin{aligned} \bar{X}_M^{(\ell, m)} &= (1 - \tau^2) \sum_{k=0}^{\ell} \sum_{n=0}^m \binom{\ell}{k} \binom{m}{n} \delta^{(k)} \delta^{(n)} f^{(\ell-k)} f^{(m-n)} \\ \bar{b}_M^{(\ell, m)} &= \tau^2 \beta_M^{(\ell, m)} + (1 - \tau^2) \sum_{k=0}^{\ell} \sum_{n=0}^m \binom{\ell}{k} \binom{m}{n} \beta_M^{(\ell-k, m-n)} \\ &\quad \times f^{(k)} f^{(n)}. \end{aligned}$$

Using these results in combination with Corollary 6, we immediately obtain the asymptotic equivalents of \mathbf{A}_k and \mathbf{B}_k :

Corollary 7. Let $\tilde{\mathbf{A}}$ and $\tilde{\mathbf{B}}$ be the $J \times J$ matrices, whose entries are

$$\begin{aligned} [\tilde{\mathbf{A}}]_{\ell, m} &= \frac{(-1)^{\ell+m} \bar{X}_M^{(\ell, m)}}{\ell! m!} \\ [\tilde{\mathbf{B}}]_{\ell, m} &= \frac{(-1)^{\ell+m} \bar{b}_M^{(\ell, m)}}{\ell! m!}. \end{aligned}$$

Then, in the asymptotic regime, for any $k \in 1, \dots, K$ we have

$$\max \left(\|\mathbf{A}_k - K p_k \tilde{\mathbf{A}}\|, \|\mathbf{B}_k - \text{tr}(\mathbf{P}) \tilde{\mathbf{B}}\| \right) \xrightarrow[M, K \rightarrow +\infty]{\text{a.s.}} 0.$$

A. Optimization of the Polynomial Coefficients

Next, we consider the optimization of the asymptotic SINRs with respect to the polynomial coefficients $\mathbf{w} = [w_0 \dots w_{J-1}]^T$. Using results from the previous sections, a deterministic equivalent for the SINR of the k th UT is

$$\gamma_k = \frac{K p_k \mathbf{w}^T \tilde{\mathbf{A}} \mathbf{w}}{\text{tr}(\mathbf{P}) \mathbf{w}^T \tilde{\mathbf{B}} \mathbf{w} + \sigma^2}.$$

The optimized TPE precoding should satisfy the power constraints in (8):

$$\text{tr}(\mathbf{G}_{\text{TPE}} \mathbf{G}_{\text{TPE}}^H) = P \quad (32)$$

or equivalently

$$\mathbf{w}^T \mathbf{C} \mathbf{w} = P \quad (33)$$

where the (ℓ, m) th element of the $J \times J$ matrix \mathbf{C} is

$$[\mathbf{C}]_{\ell, m} = \frac{1}{K} \text{tr} \left(\left(\frac{\hat{\mathbf{H}} \hat{\mathbf{H}}^H}{K} \right)^\ell \hat{\mathbf{H}} \mathbf{P} \hat{\mathbf{H}}^H \left(\frac{\hat{\mathbf{H}} \hat{\mathbf{H}}^H}{K} \right)^m \right). \quad (34)$$

In order to make the optimization problem independent of the channel realizations, we replace the constraint in (33) by a deterministic one, which depends only on the statistics of the channel. To find a deterministic equivalent of the matrix \mathbf{C} , we introduce the random quantity

$$\begin{aligned} Y_M(t, u) &= \\ &\frac{1}{K} \text{tr} \left(\left(\left(\frac{t}{K} \hat{\mathbf{H}} \hat{\mathbf{H}}^H + \mathbf{I} \right)^{-1} \hat{\mathbf{H}} \mathbf{P} \hat{\mathbf{H}}^H \left(\frac{t}{K} \hat{\mathbf{H}} \hat{\mathbf{H}}^H + \mathbf{I} \right)^{-1} \right) \right) \end{aligned}$$

whose derivatives $Y_M^{(\ell, m)}$ satisfy

$$[\mathbf{C}]_{\ell, m} = \frac{(-1)^{\ell+m} Y_M^{(\ell, m)}}{\ell! m!}.$$

Using the same method as for the matrices \mathbf{A} and \mathbf{B} , we achieve the following result:

Theorem 8. Considering the setting of Theorem 5, we have the following convergence results:

1) Let $c(t, u) = \frac{\frac{1}{K} \text{tr}(\Phi \mathbf{T}(u) \Phi \mathbf{T}(t))}{(1+t\delta(t))(1+u\delta(u))} (1+tu\beta(t, u))$, then

$$Y_M(t, u) - \text{tr}(\mathbf{P}) c(t, u) \xrightarrow[M, K \rightarrow +\infty]{\text{a.s.}} 0.$$

2) Denote by $c^{(\ell, m)}$ the ℓ th and m th derivatives with respect to t and u , respectively, then

$$\begin{aligned} c^{(\ell, m)} &= \sum_{k=1}^{\ell} \sum_{n=1}^m kn \binom{\ell}{k} \binom{m}{n} \beta^{(n-1, k-1)} \\ &\quad \times \frac{1}{K} \text{tr}(\Phi \mathcal{T}^{(\ell-k)} \mathcal{T}^{(m-n)}) + \frac{1}{K} \text{tr}(\Phi \mathcal{T}^{(m)} \mathcal{T}^{(\ell)}). \end{aligned}$$

3) Let $\tilde{\mathbf{C}}$ be the $J \times J$ matrix with entries given by

$$[\tilde{\mathbf{C}}]_{\ell, m} = \frac{(-1)^{\ell+m} c^{(\ell, m)}}{\ell! m!}.$$

Then, in the asymptotic regime

$$\|\mathbf{C} - \text{tr}(\mathbf{P}) \tilde{\mathbf{C}}\| \xrightarrow[M, K \rightarrow +\infty]{\text{a.s.}} 0.$$

Proof: Since the proof relies on the same techniques as before, we provide only a sketch in Appendix F. ■

Based on Theorem 8, we can consider the deterministic power constraint

$$\text{tr}(\mathbf{P}) \mathbf{w}^T \tilde{\mathbf{C}} \mathbf{w} = P \quad (35)$$

which can be seen as an approximation of (33), in the sense that for any \mathbf{w} satisfying (35), we have

$$\mathbf{w}^T \mathbf{C} \mathbf{w} - P \xrightarrow[M, K \rightarrow +\infty]{\text{a.s.}} 0.$$

Now the maximization of the asymptotic SINR of UT k amounts to solving the following optimization problem:

$$\begin{aligned} & \underset{\mathbf{w}}{\text{maximize}} && \frac{K p_k \mathbf{w}^H \tilde{\mathbf{A}} \mathbf{w}}{\text{tr}(\mathbf{P}) \mathbf{w}^H \tilde{\mathbf{B}} \mathbf{w} + \sigma^2} \\ & \text{subject to} && \text{tr}(\mathbf{P}) \mathbf{w}^H \tilde{\mathbf{C}} \mathbf{w} = P. \end{aligned} \quad (36)$$

The next theorem shows that the optimal solution, \mathbf{w}_{opt} , to (36) admits a closed-form expression.

Theorem 9. *Let \mathbf{a} be an eigenvector corresponding to the maximum eigenvalue λ_{\max} of*

$$\left(\tilde{\mathbf{B}} + \frac{\sigma^2}{P} \tilde{\mathbf{C}} \right)^{-\frac{1}{2}} \tilde{\mathbf{A}} \left(\tilde{\mathbf{B}} + \frac{\sigma^2}{P} \tilde{\mathbf{C}} \right)^{-\frac{1}{2}}. \quad (37)$$

Then the optimal value of the problem in (36) is achieved by

$$\mathbf{w}_{\text{opt}} = \sqrt{\frac{P}{\alpha \text{tr}(\mathbf{P})}} \left(\tilde{\mathbf{B}} + \frac{\sigma^2}{P} \tilde{\mathbf{C}} \right)^{-\frac{1}{2}} \mathbf{a} \quad (38)$$

where the scaling factor α is

$$\alpha = \left\| \tilde{\mathbf{C}}^{\frac{1}{2}} \left(\tilde{\mathbf{B}} + \frac{\sigma^2}{P} \tilde{\mathbf{C}} \right)^{-\frac{1}{2}} \mathbf{a} \right\|^2. \quad (39)$$

Moreover, for the optimal coefficients, the asymptotic SINR for the k th UT is

$$\gamma_k = \frac{K p_k \lambda_{\max}}{\text{tr}(\mathbf{P})}. \quad (40)$$

Proof: The proof is given Appendix G. ■

The optimal polynomial coefficients for UT k are given in (38) of Theorem 9. Interestingly, these coefficients are independent of the user index, thus we have indeed derived the jointly optimal coefficients. Furthermore, all users converge to the same deterministic SINR up to an UT-specific scaling factor $\frac{K p_k}{\gamma \text{tr}(\mathbf{P})}$.

Remark 1. *The asymptotic SINR expressions in (40) are only functions of the statistics and the power allocation p_1, \dots, p_K . The power allocation can be optimized with respect to some system performance metric. For example, one can show that the asymptotic average achievable rate*

$$\frac{1}{K} \sum_{k=1}^K \log_2 \left(1 + \frac{K p_k \lambda_{\max}}{\text{tr}(\mathbf{P})} \right)$$

is maximized by a uniform power allocation $p_k = \frac{P}{K}$ for all k .

Remark 2. *Theorem 9 shows that the J polynomial coefficients that jointly maximize the asymptotic SINRs can be computed using only the channel statistics. The optimal coefficients are given in closed form in (38) and are computed using approximately $\frac{J^3}{3} + 4J^2$ arithmetic operations [34]. At finite M and K , there are other coefficients that provide higher UT rates, however, these depend on the current channel estimate $\hat{\mathbf{H}}$ and thus must be recomputed in each coherence period. Hence, the main feature of Theorem 9 is that the TPE precoding coefficients can be computed beforehand, or at least be updated at with the relatively slow rate of change of the channel statistics. Thus, the cost of the optimization step is negligible with respect to calculating the precoding itself. The*

performance of finite-dimensional large-scale MIMO systems is evaluated numerically in Section VI.

Remark 3. *We have assumed the covariance matrix Φ is exactly known and estimated before the precoding is calculated. While it would be interesting to know the sensitivity of the optimization results with respect to estimation errors, finding a properly justified error model that takes into account the structure of Φ is non-trivial and therefore left for future work.*

Remark 4. *Finally, we remark that Assumption A-5 prevents us from directly analyzing the scenario where K is fixed and $M \rightarrow \infty$, but we can infer the behavior of TPE precoding based on previous works. In particular, it is known that MRT is an asymptotically optimal precoding scheme in this scenario [4]. We recall from Section III-B that TPE precoding reduces to MRT for $J = 1$. Hence, we expect the optimal coefficients to behaves as $w_0 \neq 0$ and $w_\ell \rightarrow 0$ for $\ell \geq 1$ when $M \rightarrow \infty$. In other words, we can reduce J as M grows large and still keep a fixed performance gap to RZF precoding.*

VI. SIMULATION RESULTS

In this section, we compare the RZF precoding from [16] (which was restated in (9)) with the proposed TPE precoding (defined in (18)) by means of simulations. The purpose is to validate the performance of the proposed precoding scheme and illustrate some of its main properties. The performance measure is the average achievable rate

$$r = \frac{1}{K} \sum_{k=1}^K \mathbb{E}[\log_2(1 + \text{SINR}_k)]$$

of the UTs, where the expectation is taken with respect to different channel realizations and users. In the simulations, we model the channel covariance matrix as

$$[\Phi]_{i,j} = \begin{cases} a^{j-i}, & i \leq j, \\ (a^{i-j})^*, & i > j \end{cases}$$

where a is chosen to be 0.1. This approach is known as the exponential correlation model [39]. The sum power constraint

$$\text{tr}(\mathbf{G}_{\text{RZF/TPE}} \mathbf{G}_{\text{RZF/TPE}}^H) = P$$

is applied for both precoding schemes. Unless otherwise stated, we use uniform power allocation for the UTs, since the asymptotic properties of RZF precoding are known in this case (see Theorem 3). Without loss of generality, we have set $\sigma^2 = 1$. Our default simulation model is a large-scale single-cell MIMO system of dimensions $M = 128$ and $K = 32$.

We first take a look at Fig. 3. It considers a TPE order of $J = 5$ and three different quality levels of the CSI at the BS: $\tau \in \{0.1, 0.4, 0.7\}$. From Fig. 3, we see that RZF and TPE achieve almost the same average UT performance when a bad channel estimate is available ($\tau = 0.7$). Furthermore, TPE and RZF perform almost identically at low SNR values, for any τ . In general, the unsurprising observation is that the rate difference becomes larger at high SNRs and when τ is small (i.e., with more accurate channel knowledge).

Fig. 4 shows more directly the relationship between the average achievable UT rates and the TPE order J . We consider

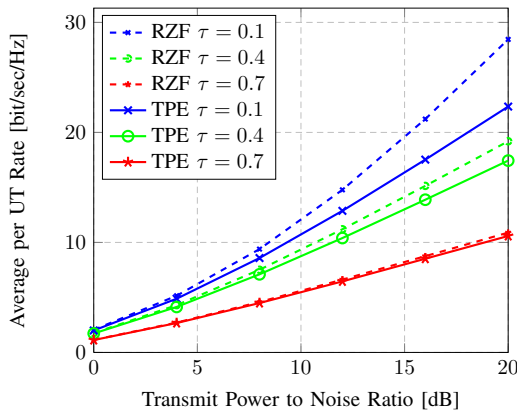


Fig. 3. Average per UT rate vs. transmit power to noise ratio for varying CSI errors at the BS ($J = 5$, $M = 128$, $K = 32$).

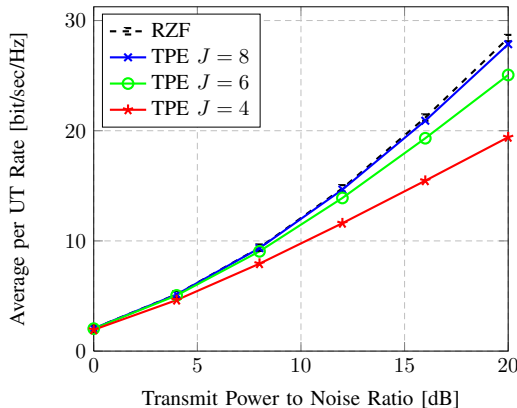


Fig. 4. Average UT rate vs. transmit power to noise ratio for different orders J in the TPE precoding ($M = 512$, $K = 128$, $\tau = 0.1$).

the case $\tau = 0.1$, $M = 512$, and $K = 128$, in order to be in a regime where TPE performs relatively bad (see Fig. 3) and the precoding complexity becomes an issue. From the figure, we see that choosing a larger value for J gives a TPE performance closer to that of RZF. However, doing so will also require more hardware; see Section IV-B. The proposed TPE precoding never surpasses the RZF performance, which is noteworthy since TPE has J degrees of freedom that can be optimized (see Section V-A), while RZF only has one design parameter. Hence one can regard RZF precoding as an upper bound to TPE precoding in the single-cell scenario.⁴

It is desirable to select the TPE order J in such a way that we achieve a certain limited rate-loss with respect RZF precoding. Fig. 5 illustrates the rate-loss (per UT) between TPE and RZF, while the number of UTs K and transmit antennas M increase with a fixed ratio ($M/K = 4$). The figure considers the case of $\tau = 0.1$. We observe, that the TPE order J and the system dimensions are independent in their respective effects on the rate-loss between TPE and RZF precoding. This observation is in line with previous results on polynomial expansions, for example [19] where reduced-rank received filtering was considered. The independence between J and the system dimensions M and K is indeed a main motivation behind TPE precoding, because it implies that the

⁴The optimal precoding parametrization in [15] has $K-1$ parameters. To optimize some general performance metric, it is therefore necessary to let the number of design parameters scale with the system dimensions.

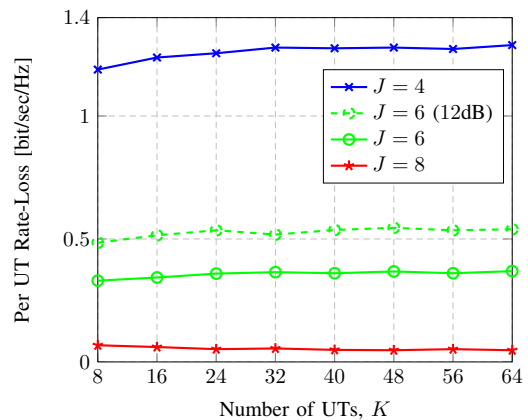


Fig. 5. Rate-loss of TPE vs. RZF with respect to growing K , where the ratio M/K is fixed at 4 and the average SNR is set to 10 dB ($\tau = 0.1$).

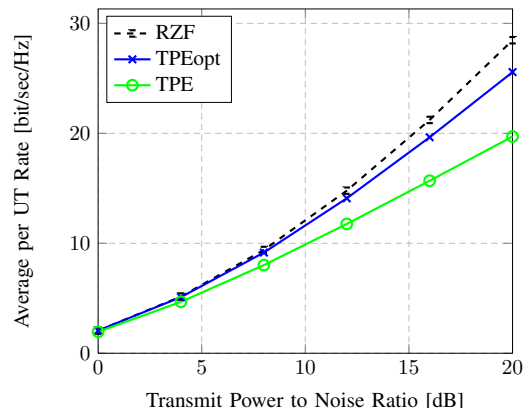


Fig. 6. Average UT rate vs. transmit power to noise ratio with RZF, TPE, and TPEopt precoding ($J = 3$, $M = 128$, $K = 32$, $\tau = 0.1$).

order J can be kept small even when TPE precoding is applied to very large-scale MIMO systems. The intuition behind this result is that the polynomial expansion approximates the inversion of each eigenvalue with the same accuracy, irrespective of the number of eigenvalues; see Section III-B for details. Although the relative performance loss is unaffected by the system dimensions, we also see that J needs to be increased along with the SNR, if a constant performance gap is desired.

In the simulation depicted in Fig. 6, we introduce a hypothetical case of TPE precoding (TPEopt) that optimizes the J coefficients using the estimated channel coefficients in each coherence period, instead of relying solely on the channel statistics. More precisely, the optimal coefficients in Theorem 9 are not computed using the deterministic equivalents of $\bar{\mathbf{A}}$, $\bar{\mathbf{B}}$, and $\bar{\mathbf{C}}$, but using the original matrices. This plot illustrates the additional performance loss caused by precalculating the TPE coefficients based on channel statistics and asymptotic analysis, instead of carrying out the optimization step for each channel realization. The difference is small at low SNRs, but noticeable at high SNRs. Furthermore, we note that increasing the value of J has the same performance-gap-reducing effect on TPEopt, as it has on TPE (see Figs. 4 and 5). In order to preserve readability, only the curves pertaining to $J = 3$ are shown in Fig. 6.

Finally, to assess the validity of our results, we treat the case of non-uniform power allocation (i.e., with different values for p_k). In particular, we considered a situation where the users

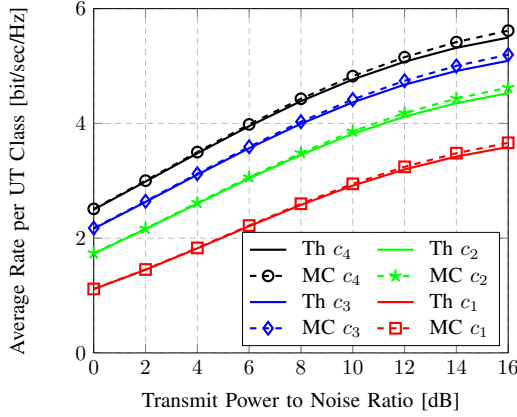


Fig. 7. Average rate per UT class vs. transmit power to noise ratio with TPE precoding ($J = 3$, $M = 128$, $K = 32$, $\tau = 0.1$).

are divided into four classes corresponding to $\{c_1, c_2, c_3, c_4\} = \{1, 2, 3, 4\}$, where $p_k = \frac{c_k}{K}$ in order to adhere to the scaling in Assumption A-4. Fig. 7 shows the theoretical (Th; based on (40)) and empirical (MC; based on (24)) average rate per UT for each class, when $K = 32$, $M = 128$, and $\tau = 0.1$. We especially remark the very good agreement between our theoretical analysis and the empirical system performance.

VII. CONCLUSION

The computational and implementation complexity of RZF precoding is prohibitively high in large-scale MIMO systems, due to the required channel matrix inversion. In this paper, we have proposed a new class of TPE precoding schemes where this inversion is approximated by truncated polynomial expansions to enable simple hardware implementation. In the single-cell downlink with M transmit antennas and K single-antenna users, this new class can approximate RZF precoding to an arbitrary accuracy by choosing the TPE order J in the interval $1 \leq J \leq \min(M, K)$. In terms of implementation complexity, TPE precoding has several advantages: 1) There is no need to compute the precoding matrix beforehand (which leaves more channel uses for data transmission); 2) the multistage structure enables parallelization and pipelining; 3) only addition and multiplication operations are required; and 4) the parameter J can be tailored to the available hardware.

Although the polynomial coefficients depend on the instantaneous channel realizations, we have shown that the per-user SINRs converge to deterministic values in the large- (M, K) regime. This enabled us to compute asymptotically optimal coefficients using merely the statistics of the channels. The simulations revealed that the difference in performance between RZF and TPE is small at low SNRs and for large CSI errors. The TPE order J can be chosen very small in these situations and, in general, it does not need to scale with the system dimensions. However, to maintain a fixed per-user rate loss compared to RZF, J should increase with the SNR or as the CSI quality improves.

Finally, we note that TPE precoding can be also applied in practical multi-cell scenarios. Our companion paper [24] provides the necessary multi-cell details, including ways to handle user-specific channel statistics, pilot contamination

(due to pilot reuse in neighboring cells), different TPE orders in different cells, cell-specific power constraints, and new ways to optimize the corresponding polynomial coefficients.

APPENDIX A USEFUL LEMMAS

Lemma 10 (Common inverses of resolvents). *Given any matrix $\hat{\mathbf{H}} \in \mathbb{C}^{M \times K}$, let $\hat{\mathbf{h}}_k$ denote its k th column and $\hat{\mathbf{H}}_k$ denote the matrix obtained after removing the k th column from $\hat{\mathbf{H}}$. The resolvent matrices of $\hat{\mathbf{H}}$ and $\hat{\mathbf{H}}_k$ are denoted by $\mathbf{Q}(t) = \left(\frac{t}{K} \hat{\mathbf{H}} \hat{\mathbf{H}}^H + \mathbf{I}_M \right)^{-1}$ and $\mathbf{Q}_k(t) = \left(\frac{t}{K} \hat{\mathbf{H}}_k \hat{\mathbf{H}}_k^H + \mathbf{I}_M \right)^{-1}$ respectively. It then holds, that*

$$\mathbf{Q}(t) = \mathbf{Q}_k(t) - \frac{1}{K} \frac{t \mathbf{Q}_k(t) \hat{\mathbf{h}}_k \hat{\mathbf{h}}_k^H \mathbf{Q}_k(t)}{1 + \frac{t}{K} \hat{\mathbf{h}}_k^H \mathbf{Q}_k(t) \hat{\mathbf{h}}_k} \quad (41)$$

and also

$$\mathbf{Q}(t) \hat{\mathbf{h}}_k = \frac{\mathbf{Q}_k(t) \hat{\mathbf{h}}_k}{1 + \frac{t}{K} \hat{\mathbf{h}}_k^H \mathbf{Q}_k(t) \hat{\mathbf{h}}_k}. \quad (42)$$

Proof: This follows from the Woodbury identity [40]. ■

The following lemma characterizes the asymptotic behavior of quadratic forms. It will be of frequent use in the computation of deterministic equivalents.

Lemma 11 (Convergence of quadratic forms). *Let $\mathbf{x}_M = [X_1, \dots, X_M]^T$ be a $M \times 1$ vector with i.i.d. complex Gaussian random variables with unit variance. Let \mathbf{A}_M be an $M \times M$ matrix independent of \mathbf{x}_M , whose spectral norm is bounded; that is, there exists $C_A < \infty$ such that $\|\mathbf{A}_M\|_2 \leq C_A$. Then, for any $p \geq 1$, there exists a constant C_p depending only on p , such that*

$$\mathbb{E}_{\mathbf{x}_M} \left[\left| \frac{1}{M} \mathbf{x}_M^H \mathbf{A}_M \mathbf{x}_M - \frac{1}{M} \text{tr}(\mathbf{A}_M) \right|^p \right] \leq \frac{C_p C_A^p}{M^{p/2}}$$

where the expectation is taken over the distribution of \mathbf{x}_M . By choosing $p \geq 2$, we thus have that

$$\frac{1}{M} \mathbf{x}_M^H \mathbf{A}_M \mathbf{x}_M - \frac{1}{M} \text{tr}(\mathbf{A}_M) \xrightarrow[M \rightarrow +\infty]{\text{a.s.}} 0.$$

Lemma 12. *Let \mathbf{A}_M be as in Lemma 11, and $\mathbf{x}_M, \mathbf{y}_M$ be random, mutually independent with complex Gaussian entries of zero mean and variance 1. Then,*

$$\frac{1}{M} \mathbf{y}_M^H \mathbf{A}_M \mathbf{x}_M \xrightarrow[M, K \rightarrow +\infty]{\text{a.s.}} 0.$$

Lemma 13 (Rank-one perturbation lemma). *Let $\mathbf{Q}(t)$ and $\mathbf{Q}_k(t)$ be the resolvent matrices as defined in Lemma 10. Then, for any matrix \mathbf{A} we have:*

$$\text{tr} \left(\mathbf{A} (\mathbf{Q}(t) - \mathbf{Q}_k(t)) \right) \leq \|\mathbf{A}\|_2.$$

Lemma 14. *Let X_M and Y_M be two scalar random variables, with variances such that $\text{var}(X_M) = \mathcal{O}(M^{-2})$ and $\text{var}(Y_M) = \mathcal{O}(M^{-2}) = \mathcal{O}(K^{-2})$. Then*

$$\mathbb{E}[X_M Y_M] = \mathbb{E}[X_M] \mathbb{E}[Y_M] + o(1).$$

Proof: We have

$$\mathbb{E}[X_M Y_M] = \mathbb{E}[(X_M - \mathbb{E}[X_M])(Y_M - \mathbb{E}[Y_M])] + \mathbb{E}[X_M] \mathbb{E}[Y_M].$$

Using the Cauchy-Schwartz inequality, we see that

$$\mathbb{E} [| (X_M - \mathbb{E}[X_M])(Y_M - \mathbb{E}[Y_M]) |] \leq \sqrt{\text{var}(X_M)\text{var}(Y_M)} = \mathcal{O}(K^{-2})$$

which establishes the desired result. \blacksquare

APPENDIX B PROOF OF THEOREM 5

Here we proof Theorem 5, which establishes the asymptotic convergence of $X_{k,M}(t, u)$ and $Z_{k,M}(t, u)$ to deterministic quantities.

A. Deterministic equivalent for $X_{k,M}(t, u)$

We will begin by treating the random quantity $X_{k,M}(t, u)$. Using the notation of Lemma 10, we can write

$$X_{k,M}(t, u) = \frac{1}{K^2} \mathbf{h}_k^H \mathbf{Q}(t) \hat{\mathbf{h}}_k \hat{\mathbf{h}}_k^H \hat{\mathbf{h}}_k^H \mathbf{Q}(u) \mathbf{h}_k.$$

To control the quadratic form $\frac{1}{K} \mathbf{h}_k^H \mathbf{Q}(t) \hat{\mathbf{h}}_k$, we need to remove the dependency of $\mathbf{Q}(t)$ on vector $\hat{\mathbf{h}}_k$. For that, we shall use the relation in (41), thereby yielding

$$\begin{aligned} \frac{1}{K} \mathbf{h}_k^H \mathbf{Q}(t) \hat{\mathbf{h}}_k &= \frac{1}{K} \mathbf{h}_k^H \mathbf{Q}_k(t) \hat{\mathbf{h}}_k \\ &\quad - \frac{t}{K^2} \frac{\mathbf{h}_k^H \mathbf{Q}_k(t) \hat{\mathbf{h}}_k \hat{\mathbf{h}}_k^H \mathbf{Q}_k(t) \hat{\mathbf{h}}_k}{1 + \frac{t}{K} \hat{\mathbf{h}}_k^H \mathbf{Q}_k(t) \hat{\mathbf{h}}_k}. \end{aligned} \quad (43)$$

Using Lemma 11, we thus have

$$\frac{1}{K} \hat{\mathbf{h}}_k^H \mathbf{Q}_k(t) \hat{\mathbf{h}}_k - \frac{1}{K} \text{tr}(\Phi \mathbf{Q}_k(t)) \xrightarrow[M, K \rightarrow +\infty]{\text{a.s.}} 0.$$

Since $\frac{1}{K} \text{tr}(\Phi \mathbf{Q}_k(t)) - \frac{1}{K} \text{tr}(\Phi \mathbf{Q}(t)) \xrightarrow[M, K \rightarrow +\infty]{\text{a.s.}} 0$, by the rank-one perturbation property in Lemma 13, we have

$$\frac{1}{K} \hat{\mathbf{h}}_k^H \mathbf{Q}_k(t) \hat{\mathbf{h}}_k - \frac{1}{K} \text{tr}(\Phi \mathbf{Q}(t)) \xrightarrow[M, K \rightarrow +\infty]{\text{a.s.}} 0.$$

Finally, Theorem 1 implies that

$$\frac{1}{K} \hat{\mathbf{h}}_k^H \mathbf{Q}_k(t) \hat{\mathbf{h}}_k - \delta(t) \xrightarrow[M, K \rightarrow +\infty]{\text{a.s.}} 0. \quad (44)$$

The same kind of calculations can be used to deal with the quadratic form $\frac{1}{K} \mathbf{h}_k^H \mathbf{Q}_k(t) \hat{\mathbf{h}}_k$, whose asymptotic limit is the same as $\frac{\sqrt{1-\tau^2}}{K} \mathbf{h}_k^H \mathbf{Q}_k(t) \hat{\mathbf{h}}_k$, due to the independence between the channel estimation error and the channel vector \mathbf{h}_k . Hence,

$$\frac{1}{K} \mathbf{h}_k^H \mathbf{Q}_k(t) \hat{\mathbf{h}}_k - \sqrt{1-\tau^2} \delta(t) \xrightarrow[M, K \rightarrow +\infty]{\text{a.s.}} 0. \quad (45)$$

Plugging the deterministic approximation of (44) and (45) into (43), we thus see that

$$\frac{1}{K} \mathbf{h}_k^H \mathbf{Q}(t) \hat{\mathbf{h}}_k - \frac{\sqrt{1-\tau^2} \delta(t)}{1+t\delta(t)} \xrightarrow[M, K \rightarrow +\infty]{\text{a.s.}} 0$$

and hence

$$X_{k,M}(t, u) - \frac{(1-\tau^2)\delta(t)\delta(u)}{1+t\delta(t)(1+u\delta(u))} \xrightarrow[M, K \rightarrow +\infty]{\text{a.s.}} 0.$$

B. Deterministic equivalent for $Z_{k,M}(t, u)$

Finding a deterministic equivalent for $Z_{k,M}(t, u)$ is much more involved than for $X_{k,M}(t, u)$. Following the same steps as in Appendix B-A, we decompose $Z_{k,M}(t, u)$ as

$$\begin{aligned} Z_{k,M}(t, u) &= \frac{1}{K} \mathbf{h}_k^H \mathbf{Q}_k(t) \hat{\mathbf{H}} \hat{\mathbf{P}} \hat{\mathbf{H}}^H \mathbf{Q}_k(u) \mathbf{h}_k \\ &\quad - \frac{\frac{u}{K^2} \mathbf{h}_k^H \mathbf{Q}_k(t) \hat{\mathbf{H}} \hat{\mathbf{P}} \hat{\mathbf{H}}^H \mathbf{Q}_k(u) \hat{\mathbf{h}}_k \hat{\mathbf{h}}_k^H \mathbf{Q}_k(u) \mathbf{h}_k}{1 + \frac{u}{K} \hat{\mathbf{h}}_k^H \mathbf{Q}_k(u) \hat{\mathbf{h}}_k} \\ &\quad - \frac{\frac{t}{K^2} \mathbf{h}_k^H \mathbf{Q}_k(t) \hat{\mathbf{h}}_k \hat{\mathbf{h}}_k^H \mathbf{Q}_k(t) \hat{\mathbf{H}} \hat{\mathbf{P}} \hat{\mathbf{H}}^H \mathbf{Q}_k(u) \mathbf{h}_k}{1 + \frac{t}{K} \hat{\mathbf{h}}_k^H \mathbf{Q}_k(t) \hat{\mathbf{h}}_k} \\ &\quad + \frac{\frac{tu}{K^3} \mathbf{h}_k^H \mathbf{Q}_k(t) \hat{\mathbf{h}}_k \hat{\mathbf{h}}_k^H \mathbf{Q}_k(t) \hat{\mathbf{H}} \hat{\mathbf{P}} \hat{\mathbf{H}}^H \mathbf{Q}_k(u) \hat{\mathbf{h}}_k \hat{\mathbf{h}}_k^H \mathbf{Q}_k(u) \mathbf{h}_k}{(1 + \frac{t}{K} \hat{\mathbf{h}}_k^H \mathbf{Q}_k(t) \hat{\mathbf{h}}_k)(1 + \frac{u}{K} \hat{\mathbf{h}}_k^H \mathbf{Q}_k(u) \hat{\mathbf{h}}_k)} \\ &\triangleq X_1(t, u) + X_2(t, u) + X_3(t, u) + X_4(t, u). \end{aligned}$$

As it will be shown next, to determine the asymptotic limit of the random variables $X_i(t, u)$, $i = 1, \dots, 4$, we need to find a deterministic equivalent for

$$\frac{1}{K} \text{tr}(\Phi \mathbf{Q}(t) \hat{\mathbf{H}} \hat{\mathbf{P}} \hat{\mathbf{H}}^H \mathbf{Q}(u)).$$

This is the most involved step of the proof. It will, thus, be treated separately in Appendix C, where we establish the following lemma:

Lemma 15. *Let \mathbf{H} be an $M \times K$ random matrix whose columns are drawn according to Assumption A-1. Define for $t \geq 0$, the resolvent matrix $\mathbf{Q}(t) = (\frac{t}{K} \mathbf{H} \mathbf{H}^H + \mathbf{I}_K)^{-1}$. Let \mathbf{A} be an $M \times M$ deterministic matrix with uniformly spectral norm and $\hat{\alpha}_M(t, u, \mathbf{A})$ given as*

$$\hat{\alpha}_M(t, u, \mathbf{A}) = \frac{1}{K} \text{tr}(\mathbf{A} \mathbf{Q}(t) \mathbf{H} \hat{\mathbf{P}} \hat{\mathbf{H}}^H \mathbf{Q}(u)).$$

Then, in the asymptotic regime described by Assumption A-5, we have

$$\hat{\alpha}_M(t, u, \mathbf{A}) - \bar{\alpha}_M(t, u, \mathbf{A}) \xrightarrow[M, K \rightarrow +\infty]{\text{a.s.}} 0$$

where

$$\begin{aligned} \bar{\alpha}_M(t, u, \mathbf{A}) &= \text{tr}(\mathbf{P}) \frac{\frac{1}{K} \text{tr}(\Phi \mathbf{T}(u) \mathbf{A} \mathbf{T}(t))}{(1+t\delta(t))(1+u\delta(u))} \\ &\quad + \frac{\text{tr}(\mathbf{P})}{(1+t\delta(t))(1+u\delta(u))} \\ &\quad \times \frac{\frac{tu}{K} \text{tr}(\Phi \mathbf{T}(u) \mathbf{A} \mathbf{T}(t)) \frac{1}{K} \text{tr}(\Phi \mathbf{T}(u) \Phi \mathbf{T}(t))}{(1+t\delta(t))(1+u\delta(u)) - \frac{tu}{K} \text{tr}(\Phi \mathbf{T}(u) \Phi \mathbf{T}(t))}. \end{aligned} \quad (46)$$

In particular, if $\mathbf{A} = \Phi$, we have

$$\bar{\alpha}_M(t, u, \Phi) = \frac{\text{tr}(\mathbf{P}) \frac{1}{K} \text{tr}(\Phi \mathbf{T}(u) \Phi \mathbf{T}(t))}{(1+t\delta(t))(1+u\delta(u)) - \frac{tu}{K} \text{tr}(\Phi \mathbf{T}(u) \Phi \mathbf{T}(t))}.$$

Let us begin by treating $X_1(t, u)$:

$$\begin{aligned} \frac{1}{K} \mathbf{h}_k^H \mathbf{Q}_k(t) \hat{\mathbf{H}} \hat{\mathbf{P}} \hat{\mathbf{H}}^H \mathbf{Q}_k(u) \mathbf{h}_k &= \frac{1}{K} \mathbf{h}_k^H \mathbf{Q}_k(t) \hat{\mathbf{H}}_k \mathbf{P}_k \hat{\mathbf{H}}_k^H \mathbf{Q}_k(u) \mathbf{h}_k \\ &\quad - \frac{p_k}{K} \mathbf{h}_k^H \mathbf{Q}_k(t) \hat{\mathbf{h}}_k \hat{\mathbf{h}}_k^H \mathbf{Q}_k(u) \mathbf{h}_k. \end{aligned}$$

The right-hand side term in the equation above can be treated using (45), thereby yielding

$$\frac{p_k}{K} \mathbf{h}_k^H \mathbf{Q}_k(t) \hat{\mathbf{h}}_k \hat{\mathbf{h}}_k^H \mathbf{Q}_k(u) \mathbf{h}_k - K p_k (1 - \tau^2) \delta(t) \delta(u) \xrightarrow[M, K \rightarrow +\infty]{\text{a.s.}} 0.$$

Using Lemma 11, we can prove that

$$\begin{aligned} & \frac{1}{K} \mathbf{h}_k^H \mathbf{Q}_k(t) \hat{\mathbf{H}}_k \mathbf{P}_k \hat{\mathbf{H}}_k^H \mathbf{Q}_k(u) \mathbf{h}_k \\ & - \frac{1}{K} \text{tr} \left(\Phi \mathbf{Q}_k(t) \hat{\mathbf{H}}_k \mathbf{P}_k \hat{\mathbf{H}}_k^H \mathbf{Q}_k(u) \right) \xrightarrow[M, K \rightarrow +\infty]{\text{a.s.}} 0. \end{aligned} \quad (47)$$

On the other hand, according to Lemma 15, we have

$$\begin{aligned} & \frac{1}{K} \text{tr} \left(\Phi \mathbf{Q}_k(t) \hat{\mathbf{H}}_k \mathbf{P}_k \hat{\mathbf{H}}_k^H \mathbf{Q}_k(u) \right) - \text{tr}(\mathbf{P}) \beta_M(t, u) \\ & \xrightarrow[M, K \rightarrow +\infty]{\text{a.s.}} 0. \end{aligned} \quad (48)$$

Combining (47) with (48) yields

$$\frac{1}{K} \mathbf{h}_k^H \mathbf{Q}_k(t) \hat{\mathbf{H}}_k \mathbf{P}_k \hat{\mathbf{H}}_k^H \mathbf{Q}_k(u) \mathbf{h}_k - \text{tr}(\mathbf{P}) \beta_M(t, u) \xrightarrow[M, K \rightarrow +\infty]{\text{a.s.}} 0.$$

Furthermore, in the asymptotic regime we have

$$X_1(t, u) - (K p_k (1 - \tau^2) \delta(t) \delta(u) + \text{tr}(\mathbf{P}) \beta_M(t, u)) \xrightarrow[M, K \rightarrow +\infty]{\text{a.s.}} 0. \quad (49)$$

Controlling the other terms $X_i(t, u)$, $i = 2, 3, 4$, will also include the term $\beta(t, u)$. First note that $X_2(t, u)$ is given by

$$X_2(t, u) = -u Y_2(t, u) \frac{\frac{1}{K} \hat{\mathbf{h}}_k^H \mathbf{Q}_k(u) \mathbf{h}_k}{1 + \frac{u}{K} \hat{\mathbf{h}}_k^H \mathbf{Q}_k(u) \hat{\mathbf{h}}_k}$$

where

$$Y_2(t, u) = \frac{1}{K} \mathbf{h}_k^H \mathbf{Q}_k(t) \hat{\mathbf{H}} \mathbf{P} \hat{\mathbf{H}}^H \mathbf{Q}_k(u) \hat{\mathbf{h}}_k.$$

Observe that $Y_2(t, u)$ is very similar to $X_2(t, u)$. The only difference is that $Y_2(t, u)$ is a quadratic form involving vectors \mathbf{h}_k and $\hat{\mathbf{h}}_k$ whereas $X_2(t, u)$ involves only the vector \mathbf{h}_k . Following the same kind of calculations leads to

$$Y_2(t, u) - \left(K p_k \sqrt{1 - \tau^2} \delta(t) \delta(u) + \sqrt{1 - \tau^2} \text{tr}(\mathbf{P}) \beta_M(t, u) \right) \xrightarrow[M, K \rightarrow +\infty]{\text{a.s.}} 0.$$

Since $\frac{\frac{1}{K} \hat{\mathbf{h}}_k^H \mathbf{Q}_k(u) \mathbf{h}_k}{1 + \frac{u}{K} \hat{\mathbf{h}}_k^H \mathbf{Q}_k(u) \hat{\mathbf{h}}_k}$ satisfies

$$\frac{\frac{1}{K} \hat{\mathbf{h}}_k^H \mathbf{Q}_k(u) \mathbf{h}_k}{1 + \frac{u}{K} \hat{\mathbf{h}}_k^H \mathbf{Q}_k(u) \hat{\mathbf{h}}_k} - \frac{\sqrt{1 - \tau^2} \delta(u)}{1 + u \delta(u)} \xrightarrow[M, K \rightarrow +\infty]{\text{a.s.}} 0$$

we now have

$$X_2(t, u) + \frac{u \delta(u) (K p_k (1 - \tau^2) \delta(t) \delta(u) + (1 - \tau^2) \text{tr}(\mathbf{P}) \beta_M(t, u))}{1 + u \delta(u)} \xrightarrow[M, K \rightarrow +\infty]{\text{a.s.}} 0. \quad (50)$$

Similarly, $X_3(t, u)$ satisfies

$$X_3(t, u) + \frac{t \delta(t) (K p_k (1 - \tau^2) \delta(t) \delta(u) + (1 - \tau^2) \text{tr}(\mathbf{P}) \beta_M(t, u))}{1 + t \delta(t)} \xrightarrow[M, K \rightarrow +\infty]{\text{a.s.}} 0. \quad (51)$$

Finally, $X_4(t, u)$ can be treated using the same approach, thereby providing the following convergence:

$$X_4(t, u) - \frac{t u \delta(t) \delta(u) ((1 - \tau^2) K p_k \delta(t) \delta(u) + \text{tr}(\mathbf{P}) \beta_M(t, u))}{(1 + t \delta(t))(1 + u \delta(u))} \xrightarrow[M, K \rightarrow +\infty]{\text{a.s.}} 0. \quad (52)$$

Summing (49), (50), (51), (52) yields

$$\begin{aligned} & Z_{k,M}(t, u) - \left(\frac{K p_k (1 - \tau^2) \delta(t) \delta(u)}{(1 + t \delta(t))(1 + u \delta(u))} \right. \\ & \left. + \text{tr}(\mathbf{P}) \left(\tau^2 + \frac{(1 - \tau^2)}{(1 + u \delta(u))(1 + t \delta(t))} \right) \beta_M(t, u) \right) \xrightarrow[M, K \rightarrow +\infty]{\text{a.s.}} 0. \end{aligned}$$

APPENDIX C PROOF OF LEMMA 15

The aim of this section is to determine a deterministic equivalent for the random quantity

$$\hat{\alpha}_M(t, u, \mathbf{A}) = \frac{1}{K} \text{tr}(\mathbf{A} \mathbf{Q}(t) \mathbf{H} \mathbf{P} \mathbf{H}^H \mathbf{Q}(u)).$$

The proof is technical and will make frequent use of results from Appendix A. First, we need to control $\text{var}(\hat{\alpha}_M(t, u))$. This has already been treated in [10] where it was proved that $\text{var}(\hat{\alpha}_M(t, u, \mathbf{A})) = \mathcal{O}(K^{-2})$ when $t = u$. The same calculations hold for $t \neq u$, thus we consider in the sequel that $\text{var}(\hat{\alpha}_M(t, u, \mathbf{A})) = \mathcal{O}(K^{-2})$. Hence, we have

$$\hat{\alpha}_M(t, u, \mathbf{A}) - \mathbb{E}[\hat{\alpha}_M(t, u, \mathbf{A})] \xrightarrow[M, K \rightarrow +\infty]{\text{a.s.}} 0. \quad (53)$$

Equation (53) allows us to focus directly on controlling $\mathbb{E}[\hat{\alpha}_M(t, u, \mathbf{A})]$. Using the resolvent identity

$$\begin{aligned} \mathbf{Q}(t) - \mathbf{T}(t) &= \mathbf{T}(t) (\mathbf{T}^{-1}(t) - \mathbf{Q}^{-1}(t)) \mathbf{Q}(t) \\ &= \mathbf{T}(t) \left(\frac{t \Phi}{1 + t \delta(t)} - \frac{t}{K} \mathbf{H} \mathbf{H}^H \right) \mathbf{Q}(t) \end{aligned}$$

we decompose $\hat{\alpha}_M(t, u, \mathbf{A})$ as

$$\begin{aligned} \hat{\alpha}_M(t, u, \mathbf{A}) &= \frac{1}{K} \text{tr}(\mathbf{A} \mathbf{T}(t) \mathbf{H} \mathbf{P} \mathbf{H}^H \mathbf{Q}(u)) \\ &+ \frac{t \text{tr}(\mathbf{A} \mathbf{T}(t) \Phi \mathbf{Q}(t) \mathbf{H} \mathbf{P} \mathbf{H}^H \mathbf{Q}(u))}{K(1 + t \delta(t))} \\ &- \frac{t}{K^2} \text{tr}(\mathbf{A} \mathbf{T}(t) \mathbf{H} \mathbf{H}^H \mathbf{Q}(t) \mathbf{H} \mathbf{P} \mathbf{H}^H \mathbf{Q}(u)) \\ &= Z_1 + Z_2 + Z_3. \end{aligned}$$

We will only directly deal with the terms Z_1 and Z_3 , since Z_2 will be compensated by terms in Z_3 . We begin with Z_1 :

$$\begin{aligned} \mathbb{E}[Z_1] &= \frac{1}{K} \sum_{\ell=1}^K p_\ell \mathbb{E}[\text{tr}(\mathbf{A} \mathbf{T}(t) \mathbf{h}_\ell \mathbf{h}_\ell^H \mathbf{Q}(u))] \\ &= \frac{1}{K} \sum_{\ell=1}^K p_\ell \mathbb{E} \left[\frac{\mathbf{h}_\ell^H \mathbf{Q}_\ell(u) \mathbf{A} \mathbf{T}(t) \mathbf{h}_\ell}{1 + \frac{u}{K} \mathbf{h}_\ell^H \mathbf{Q}_\ell(u) \mathbf{h}_\ell} \right] \\ &= \sum_{\ell=1}^K \frac{p_\ell}{K} \mathbb{E} \left[\frac{\mathbf{h}_\ell^H \mathbf{Q}_\ell(u) \mathbf{A} \mathbf{T}(t) \mathbf{h}_\ell \left(\frac{u}{K} \text{tr}(\Phi \mathbf{Q}_\ell) - \frac{u}{K} \mathbf{h}_\ell^H \mathbf{Q}_\ell(u) \mathbf{h}_\ell \right)}{(1 + \frac{u}{K} \mathbf{h}_\ell^H \mathbf{Q}_\ell(u) \mathbf{h}_\ell) (1 + \frac{u}{K} \text{tr} \Phi \mathbf{Q}_\ell(u))} \right] \\ &\quad + \frac{p_\ell}{K} \mathbb{E} \left[\frac{\mathbf{h}_\ell^H \mathbf{Q}_\ell(u) \mathbf{A} \mathbf{T}(t) \mathbf{h}_\ell}{1 + \frac{u}{K} \text{tr} \Phi \mathbf{Q}_\ell(u)} \right]. \end{aligned}$$

Using Lemma 11, we can show that the first term on the right hand side of the above equation is negligible. Therefore,

$$\begin{aligned}\mathbb{E}[Z_1] &= \sum_{\ell=1}^K \frac{p_\ell}{K} \mathbb{E} \left[\frac{\mathbf{h}_\ell^H \mathbf{Q}_\ell(u) \mathbf{A} \mathbf{T}(t) \mathbf{h}_\ell}{1 + \frac{u}{K} \text{tr}(\Phi \mathbf{Q}_\ell(u))} \right] + o(1) \\ &= \sum_{\ell=1}^K \frac{p_\ell}{K} \mathbb{E} \left[\frac{\text{tr}(\Phi \mathbf{Q}_\ell(u) \mathbf{A} \mathbf{T}(t))}{1 + \frac{u}{K} \text{tr}(\Phi \mathbf{Q}_\ell(u))} \right] + o(1).\end{aligned}$$

Using Lemma 13, we have

$$E[Z_1] = \sum_{\ell=1}^K \frac{p_\ell}{K} \mathbb{E} \left[\frac{\text{tr}(\Phi \mathbf{Q}(u) \mathbf{A} \mathbf{T}(t))}{1 + \frac{u}{K} \text{tr}(\Phi \mathbf{Q}(u))} \right] + o(1).$$

Theorem 1, thus, implies

$$\begin{aligned}E[Z_1] &= \sum_{\ell=1}^K \frac{p_\ell}{K} \mathbb{E} \left[\frac{\text{tr}(\Phi \mathbf{T}(u) \mathbf{A} \mathbf{T}(t))}{1 + u\delta(u)} \right] + o(1) \\ &= \frac{1}{K} \text{tr}(\mathbf{P}) \frac{1}{K} \text{tr}(\Phi \mathbf{T}(u) \mathbf{A} \mathbf{T}(t)) + o(1).\end{aligned}$$

We now look at Z_3 , where

$$Z_3 = -\frac{t}{K^2} \sum_{\ell=1}^K \text{tr}(\mathbf{A} \mathbf{T}(t) \mathbf{h}_\ell \mathbf{h}_\ell^H \mathbf{Q}_\ell(t) \mathbf{H} \mathbf{P} \mathbf{H}^H \mathbf{Q}(u)).$$

Using (42), we arrive at

$$Z_3 = -\frac{t}{K^2} \sum_{\ell=1}^K \frac{\text{tr}(\mathbf{A} \mathbf{T}(t) \mathbf{h}_\ell \mathbf{h}_\ell^H \mathbf{Q}_\ell(t) \mathbf{H} \mathbf{P} \mathbf{H}^H \mathbf{Q}(u))}{1 + \frac{t}{K} \mathbf{h}_\ell^H \mathbf{Q}_\ell(t) \mathbf{h}_\ell}.$$

From (41), Z_3 can be decomposed as

$$\begin{aligned}Z_3 &= -\frac{t}{K^2} \sum_{\ell=1}^K \frac{\text{tr}(\mathbf{A} \mathbf{T}(t) \mathbf{h}_\ell \mathbf{h}_\ell^H \mathbf{Q}_\ell(t) \mathbf{H} \mathbf{P} \mathbf{H}^H \mathbf{Q}_\ell(u))}{1 + \frac{t}{K} \mathbf{h}_\ell^H \mathbf{Q}_\ell(t) \mathbf{h}_\ell} \\ &\quad + \frac{tu}{K^3} \sum_{\ell=1}^K \frac{\text{tr}(\mathbf{A} \mathbf{T}(t) \mathbf{h}_\ell \mathbf{h}_\ell^H \mathbf{Q}_\ell(t) \mathbf{H} \mathbf{P} \mathbf{H}^H \mathbf{Q}_\ell(u) \mathbf{h}_\ell \mathbf{h}_\ell^H \mathbf{Q}_\ell(u))}{(1 + \frac{t}{K} \mathbf{h}_\ell^H \mathbf{Q}_\ell(t) \mathbf{h}_\ell)(1 + \frac{u}{K} \mathbf{h}_\ell^H \mathbf{Q}_\ell(u) \mathbf{h}_\ell)} \\ &= Z_{31} + Z_{32}.\end{aligned}$$

We sequentially deal with the terms Z_{31} and Z_{32} . The same arguments as those used before, allow us to substitute the denominator by $1+t\delta(t)$, thereby yielding:

$$\begin{aligned}\mathbb{E}[Z_{31}] &= -\frac{t}{K^2} \sum_{\ell=1}^K \mathbb{E} \left[\frac{\mathbf{h}_\ell^H \mathbf{Q}_\ell(t) \mathbf{H} \mathbf{P} \mathbf{H}^H \mathbf{Q}_\ell(u) \mathbf{A} \mathbf{T}(t) \mathbf{h}_\ell}{1+t\delta(t)} \right] + o(1) \\ &= -\frac{t}{K^2} \left(\sum_{\ell=1}^K \mathbb{E} \left[\frac{\mathbf{h}_\ell^H \mathbf{Q}_\ell(t) \mathbf{H}_\ell \mathbf{P}_\ell \mathbf{H}_\ell^H \mathbf{Q}_\ell(u) \mathbf{A} \mathbf{T}(t) \mathbf{h}_\ell}{1+t\delta(t)} \right] \right. \\ &\quad \left. + p_\ell \mathbb{E} \left[\frac{\mathbf{h}_\ell^H \mathbf{Q}_\ell(t) \mathbf{h}_\ell \mathbf{h}_\ell^H \mathbf{Q}_\ell(u) \mathbf{A} \mathbf{T}(t) \mathbf{h}_\ell}{1+t\delta(t)} \right] \right) + o(1) \\ &= -\frac{t}{K^2} \left(\sum_{\ell=1}^K \mathbb{E} \left[\frac{\text{tr}(\Phi \mathbf{Q}_\ell(t) \mathbf{H}_\ell \mathbf{P}_\ell \mathbf{H}_\ell^H \mathbf{Q}_\ell(u) \mathbf{A} \mathbf{T}(t))}{1+t\delta(t)} \right] \right. \\ &\quad \left. + p_\ell \mathbb{E} \left[\frac{\mathbf{h}_\ell^H \mathbf{Q}_\ell(t) \mathbf{h}_\ell \mathbf{h}_\ell^H \mathbf{Q}_\ell(u) \mathbf{A} \mathbf{T}(t) \mathbf{h}_\ell}{1+t\delta(t)} \right] \right) + o(1) \\ &\triangleq \chi_1 + \chi_2.\end{aligned}$$

By Lemma 11, the quadratic forms involved in χ_2 have variance $\mathcal{O}(K^{-2})$, and thus can be substituted by their expected mean (see Lemma 14). We obtain

$$\begin{aligned}\chi_2 &= -t \sum_{\ell=1}^K p_\ell \mathbb{E} \left[\frac{\frac{1}{K} \text{tr}(\Phi \mathbf{Q}_\ell(t)) \frac{1}{K} \text{tr}(\Phi \mathbf{Q}_\ell(u) \mathbf{A} \mathbf{T}(t))}{1+t\delta(t)} \right] + o(1) \\ &= -\frac{t\delta(t)}{1+t\delta(t)} \text{tr}(\mathbf{P}) \frac{1}{K} \text{tr}(\Phi \mathbf{T}(u) \mathbf{A} \mathbf{T}(t)) + o(1).\end{aligned}\quad (54)$$

The term χ_1 will be compensated by Z_2 . To see that, observe that the first order of χ_1 does not change if we substitute \mathbf{H}_ℓ by \mathbf{H} and \mathbf{P}_ℓ by \mathbf{P} . Besides, due to Lemma 13, we can substitute $\mathbf{Q}_\ell(t)$ by $\mathbf{Q}(t)$ and $\mathbf{Q}_\ell(u)$ by $\mathbf{Q}(u)$, hence proving that

$$\chi_1 = -\mathbb{E}[Z_2] + o(1). \quad (55)$$

Finally, it remains to deal with Z_{32} . Substituting $\frac{1}{K} \mathbf{h}_\ell^H \mathbf{Q}_\ell(t) \mathbf{h}_\ell$ and $\frac{1}{K} \mathbf{h}_\ell^H \mathbf{Q}_\ell(u) \mathbf{h}_\ell$ by their asymptotic equivalent $\delta(t)$ and $\delta(u)$, we get

$$\begin{aligned}\mathbb{E}[Z_{32}] &= \frac{tu}{K^3} \sum_{\ell=1}^K \mathbb{E} \left[\frac{\mathbf{h}_\ell^H \mathbf{Q}_\ell(u) \mathbf{A} \mathbf{T}(t) \mathbf{h}_\ell \mathbf{h}_\ell^H \mathbf{Q}_\ell(t) \mathbf{H}_\ell \mathbf{P}_\ell \mathbf{H}_\ell^H \mathbf{Q}_\ell(u) \mathbf{h}_\ell}{(1+t\delta(t))(1+u\delta(u))} \right] + \\ &\quad \frac{tu}{K^3} \sum_{\ell=1}^K p_\ell \mathbb{E} \left[\frac{\mathbf{h}_\ell^H \mathbf{Q}_\ell(u) \mathbf{A} \mathbf{T}(t) \mathbf{h}_\ell \mathbf{h}_\ell^H \mathbf{Q}_\ell(t) \mathbf{h}_\ell \mathbf{h}_\ell^H \mathbf{Q}_\ell(u) \mathbf{h}_\ell}{(1+t\delta(t))(1+u\delta(u))} \right] + o(1).\end{aligned}$$

Analogously to before, $\mathbb{E}[Z_{32}]$ can be simplified:

$$\begin{aligned}\mathbb{E}[Z_{32}] &= \frac{tu}{K^3} \sum_{\ell=1}^K \mathbb{E} \left[\frac{\text{tr}(\Phi \mathbf{Q}(t) \mathbf{H} \mathbf{P} \mathbf{H}^H \mathbf{Q}(u)) \text{tr}(\Phi \mathbf{T}(u) \mathbf{A} \mathbf{T}(t))}{(1+t\delta(t))(1+u\delta(u))} \right] \\ &\quad + \frac{tu}{K} \sum_{\ell=1}^K \frac{p_\ell \delta(t) \delta(u) \text{tr}(\Phi \mathbf{T}(u) \mathbf{A} \mathbf{T}(t))}{(1+t\delta(t))(1+u\delta(u))} + o(1) \\ &= \frac{tu}{K} \frac{\text{tr}(\Phi \mathbf{T}(u) \mathbf{A} \mathbf{T}(t)) \mathbb{E}[\hat{\alpha}_M(t, u, \Phi)]}{(1+t\delta(t))(1+u\delta(u))} \\ &\quad + \frac{\delta(t) \delta(u) \text{tr}(\mathbf{P}) \frac{tu}{K} \text{tr}(\Phi \mathbf{T}(u) \mathbf{A} \mathbf{T}(t))}{(1+t\delta(t))(1+u\delta(u))} + o(1).\end{aligned}\quad (56)$$

Combining (54), (55) and (56), we obtain

$$\begin{aligned}\mathbb{E}[\hat{\alpha}_M(t, u, \mathbf{A})] &= \frac{\text{tr}(\mathbf{P}) \frac{1}{K} \text{tr}(\Phi \mathbf{T}(u) \mathbf{A} \mathbf{T}(t))}{(1+t\delta(t))(1+u\delta(u))} \\ &\quad + \frac{tu}{K} \frac{\text{tr}(\Phi \mathbf{T}(u) \mathbf{A} \mathbf{T}(t)) \mathbb{E}[\hat{\alpha}_M(t, u, \Phi)]}{1+t\delta(t)} + o(1).\end{aligned}\quad (57)$$

Replacing \mathbf{A} with Φ , one finds a deterministic equivalent

$$\begin{aligned}\mathbb{E}[\hat{\alpha}_M(t, u, \Phi)] &= \frac{\text{tr}(\mathbf{P}) \frac{1}{K} \text{tr}(\Phi \mathbf{T}(u) \Phi \mathbf{T}(t))}{(1+t\delta(t))(1+u\delta(u)) - \frac{tu}{K} \text{tr}(\Phi \mathbf{T}(u) \Phi \mathbf{T}(t))} + o(1).\end{aligned}\quad (58)$$

Finally, substituting (58) into (57) establishes (46).

APPENDIX D PROOF OF COROLLARY 6

The proof of Corollary 6 relies on Montel's theorem [41]. We only prove the result for $X_{k,M}(t, u)$, $Z_{k,M}(t, u)$ follows analogously. Note, that $X_{k,M}(t, u)$ and $\bar{X}_{k,M}(t, u)$ are analytic functions, when their domains are extended to $\mathbb{C} \setminus \mathbb{R}_- \times$

$\mathbb{C} \setminus \mathbb{R}_-$, where \mathbb{R}_- is the set of negative real-valued numbers. Since $X_{k,M}(t, u) - \bar{X}_{k,M}(t, u)$ is almost surely bounded for large M and K on every compact subset of $\mathbb{C} \setminus \mathbb{R}_-$, Montel's theorem asserts that there exists a converging subsequence, which converges to an analytic function. Since this limiting function is necessarily zero on the positive real axis, it must be zero everywhere. Thus, from every subsequence one can extract a convergent one that converges to zero, thus

$$X_{k,M}(z_1, z_2) - \bar{X}_{k,M}(z_1, z_2) \xrightarrow[M, K \rightarrow +\infty]{\text{a.s.}} 0 \quad \forall z_1, z_2 \in \mathbb{C} \setminus \mathbb{R}_- \quad (59)$$

As $X_{k,M}(z_1, z_2)$ is analytic, the derivatives of $X_{k,M}(z_1, z_2) - \bar{X}_{k,M}(z_1, z_2)$ converge to zero. In particular, if \tilde{t} and \tilde{u} are strictly positive scalars, we have

$$X_{k,M}^{(m,\ell)}(\tilde{t}, \tilde{u}) - \bar{X}_{k,M}^{(m,\ell)}(\tilde{t}, \tilde{u}) \xrightarrow[M, K \rightarrow +\infty]{\text{a.s.}} 0. \quad (60)$$

This result can be extended to the case of $\tilde{t} = 0$ and $\tilde{u} = 0$. To see this, let $\eta > 0$ and decompose

$$X_{k,M}^{(m,\ell)} - \bar{X}_{k,M}^{(m,\ell)} = \alpha_1 + \alpha_2 + \alpha_3$$

where

$$\begin{aligned} \alpha_1 &= X_{k,M}^{(m,\ell)} - X_{k,M}^{(m,\ell)}(\eta, \eta) \\ \alpha_2 &= X_{k,M}^{(m,\ell)}(\eta, \eta) - \bar{X}_{k,M}^{(m,\ell)}(\eta, \eta) \\ \alpha_3 &= \bar{X}_{k,M}^{(m,\ell)}(\eta, \eta) - \bar{X}_{k,M}^{(m,\ell)}. \end{aligned}$$

Now, let $\epsilon > 0$. Since the derivatives of $X_{k,M}^{(m,\ell)}$ and $\bar{X}_{k,M}^{(m,\ell)}$ are almost surely bounded for large M and K , the quantities $|\alpha_1|$ and $|\alpha_3|$ can be made smaller than $\epsilon/3$ when η is small enough. On the other hand, (60) implies that α_2 converges to zero almost surely. There exists M_0 , such that, for $M \geq M_0$ we have $|\alpha_2| \leq \frac{\epsilon}{3}$. Therefore, for M large enough, $|X_{k,M}^{(m,\ell)} - \bar{X}_{k,M}^{(m,\ell)}| \leq \epsilon$, thereby proving

$$X_{k,M}^{(m,\ell)} - \bar{X}_{k,M}^{(m,\ell)} \xrightarrow[M, K \rightarrow +\infty]{\text{a.s.}} 0.$$

APPENDIX E

ITERATIVE ALGORITHM FOR COMPUTING $\beta_M^{(\ell,m)}$

An iterative approach for computing $\beta_M^{(\ell,m)}$ is given by

Algorithm 1 Iterative algorithm for the computation of $\beta_M^{(\ell,m)}$

```

for  $k = 0 \rightarrow J$  do
   $\beta_M^{(k,0)} \leftarrow \frac{1}{K} \text{tr}(\Phi \mathcal{T}^{(k)} \Phi)$ ,  $\beta_M^{(0,k)} \leftarrow \frac{1}{K} \text{tr}(\Phi \mathcal{T}^{(k)} \Phi)$ 
end for
for  $m = 1 \rightarrow J$  do
  for  $k = 1 \rightarrow J$  do
     $\beta_M^{(k,m)} \leftarrow \frac{1}{K} \text{tr}(\Phi \mathcal{T}^{(k)} \Phi \mathcal{T}^{(m)} \Phi)$ 
    for  $p_k = 1 \rightarrow k$  do
      for  $q_m = 1 \rightarrow m$  do
         $\beta_M^{(k,m)} \leftarrow \beta_M^{(k,m)} - p_k q_m \binom{k}{p_k} \binom{m}{q_m} \beta_M^{(p_k-1, q_m-1)} \frac{1}{K} \text{tr}(\Phi \mathcal{T}^{(k-p_k)} \Phi \mathcal{T}^{(m-q_m)})$ 
      end for
    end for
  end for
end for

```

APPENDIX F

SKETCH OF THE PROOF OF THEOREM 8

The goal of this section is to provide an outline of the proof for finding the deterministic equivalent of the quantity

$$[\tilde{\mathbf{C}}]_{\ell,m} = \frac{1}{K} \text{tr} \left(\left(\frac{\hat{\mathbf{H}} \hat{\mathbf{H}}^H}{K} \right)^\ell \hat{\mathbf{H}} \mathbf{P} \hat{\mathbf{H}}^H \left(\frac{\hat{\mathbf{H}} \hat{\mathbf{H}}^H}{K} \right)^m \right).$$

A full proof proceeds in the following steps:

- 1) First compute the deterministic equivalent for

$$Y_M(t, u) = \frac{1}{K} \text{tr} \left(\mathbf{Q}(t) \hat{\mathbf{H}} \mathbf{P} \hat{\mathbf{H}}^H \mathbf{Q}(u) \right)$$

where $\mathbf{Q}(t) = \left(\frac{t}{K} \mathbf{H} \mathbf{H}^H + \mathbf{I} \right)^{-1}$. This can be achieved by using Lemma 15, where it is proved that

$$Y_M(t, u) - \bar{\alpha}_M(t, u, \mathbf{I}) \xrightarrow[M, K \rightarrow +\infty]{\text{a.s.}} 0$$

and thus

$$Y_M(t, u) - \text{tr}(\mathbf{P}) c(t, u) \xrightarrow[M, K \rightarrow +\infty]{\text{a.s.}} 0.$$

- 2) Now, since

$$[\tilde{\mathbf{C}}]_{\ell,m} = \frac{(-1)^{\ell+m} Y_M^{(\ell,m)}}{\ell! m!}$$

we can prove, using the same approach as in the proof of Theorem 6, that

$$Y_M(t, u)^{(\ell,m)} - \text{tr}(\mathbf{P}) c^{(\ell,m)} \xrightarrow[M, K \rightarrow +\infty]{\text{a.s.}} 0.$$

- 3) Finally, one computes the derivative of $c(t, u)$ at $t = 0$ and $u = 0$, using the Leibniz rule, to arrive at the desired result.

APPENDIX G

PROOF OF THEOREM 9

By using that $\frac{\text{tr}(\mathbf{P}) \mathbf{w}^H \tilde{\mathbf{C}} \mathbf{w}}{P} = 1$ and dividing the objective function by the constant $\frac{K p_k}{\text{tr}(\mathbf{P})}$, the problem (36) can be rewritten as

$$\begin{aligned} (P_1) : \underset{\mathbf{w}}{\text{maximize}} \quad & \frac{\mathbf{w}^H \tilde{\mathbf{A}} \mathbf{w}}{\mathbf{w}^H \tilde{\mathbf{B}} \mathbf{w} + \frac{\sigma^2}{P} \mathbf{w}^H \tilde{\mathbf{C}} \mathbf{w}} \\ \text{subject to} \quad & \mathbf{w}^H \tilde{\mathbf{C}} \mathbf{w} = \frac{P}{\text{tr}(\mathbf{P})}. \end{aligned} \quad (61)$$

Making the change of variable $\mathbf{a} = \left(\tilde{\mathbf{B}} + \frac{\sigma^2}{P} \tilde{\mathbf{C}} \right)^{\frac{1}{2}} \mathbf{w}$, we transform (P_1) into

$$\begin{aligned} (P_2) : \quad & \underset{\mathbf{a}}{\text{maximize}} \quad \frac{\mathbf{a}^H \left(\tilde{\mathbf{B}} + \frac{\sigma^2}{P} \tilde{\mathbf{C}} \right)^{-\frac{1}{2}} \tilde{\mathbf{A}} \left(\tilde{\mathbf{B}} + \frac{\sigma^2}{P} \tilde{\mathbf{C}} \right)^{-\frac{1}{2}} \mathbf{a}}{\mathbf{a}^H \mathbf{a}} \\ \text{s.t.} \quad & \mathbf{a}^H \left(\tilde{\mathbf{B}} + \frac{\sigma^2}{P} \tilde{\mathbf{C}} \right)^{-\frac{1}{2}} \tilde{\mathbf{C}} \left(\tilde{\mathbf{B}} + \frac{\sigma^2}{P} \tilde{\mathbf{C}} \right)^{-\frac{1}{2}} \mathbf{a} = \frac{P}{\text{tr}(\mathbf{P})}. \end{aligned}$$

We notice that the objective function of (P_2) is independent of the norm of \mathbf{a} . We can, therefore, select \mathbf{a} to maximize the objective function and then adapt the norm to fit the constraint. If we discard the constraint, what remains is a

classic Rayleigh quotient [42], which is maximized by the eigenvector \mathbf{a} corresponding to the maximum eigenvalue of

$$\left(\tilde{\mathbf{B}} + \frac{\sigma^2}{P} \tilde{\mathbf{C}} \right)^{-\frac{1}{2}} \tilde{\mathbf{A}} \left(\tilde{\mathbf{B}} + \frac{\sigma^2}{P} \tilde{\mathbf{C}} \right)^{-\frac{1}{2}}.$$

By transforming \mathbf{a} back to the original variable \mathbf{w} we obtain (38), where the scaling in (39) corresponds to a scaling of \mathbf{a} in order to satisfy the constraint.

REFERENCES

- [1] Cisco, "Cisco visual networking index: Global mobile data traffic forecast update, 2012-2017," *White Paper*, 2013.
- [2] J. Hoydis, M. Kobayashi, and M. Debbah, "Green small-cell networks," *IEEE Veh. Technol. Mag.*, vol. 6, no. 1, pp. 37–43, Mar. 2011.
- [3] T.L. Marzetta, "Noncooperative cellular wireless with unlimited numbers of base station antennas," *IEEE Trans. Commun.*, vol. 9, no. 11, pp. 3590–3600, Nov. 2010.
- [4] F. Rusek, D. Persson, B.K. Lau, E.G. Larsson, T.L. Marzetta, O. Edfors, and F. Tufvesson, "Scaling up MIMO: Opportunities and challenges with very large arrays," *IEEE Signal Process. Mag.*, vol. 30, no. 1, pp. 40–60, Jan. 2013.
- [5] J. Hoydis, S. ten Brink, and M. Debbah, "Massive MIMO in the UL/DL of cellular networks: How many antennas do we need?," *IEEE J. Sel. Areas Commun.*, vol. 31, no. 2, pp. 160–171, Feb. 2013.
- [6] K. Hosseini, J. Hoydis, S. ten Brink, and M. Debbah, "Massive MIMO and small cells: How to densify heterogeneous networks," in *Proc. IEEE Int. Conf. Commun. (ICC)*, 2013.
- [7] E. Björnson, M. Kountouris, and M. Debbah, "Massive MIMO and small cells: Improving energy efficiency by optimal soft-cell coordination," in *Proc. Int. Conf. Telecommun. (ICT)*, 2013.
- [8] X. Gao, O. Edfors, F. Rusek, and F. Tufvesson, "Linear pre-coding performance in measured very-large MIMO channels," in *Proc. IEEE Veh. Tech. Conf. (VTC-Fall)*, 2011.
- [9] J. Hoydis, C. Hoek, T. Wild, and S. ten Brink, "Channel measurements for large antenna arrays," in *Int. Symp. Wireless Commun. Systems (ISWCS)*, 2012.
- [10] W. Hachem, O. Khorunzhy, P. Loubaton, J. Najim, and L. A. Pastur, "A new approach for capacity analysis of large dimensional multi-antenna channels," *IEEE Trans. Inf. Theory*, vol. 54, no. 9, pp. 3987–4004, Sept. 2008.
- [11] V.K. Nguyen and J. Evans, "Multiuser transmit beamforming via regularized channel inversion: A large system analysis," in *Proc. IEEE Global Commun. Conf. (GLOBECOM)*, 2008.
- [12] S. Wagner, R. Couillet, M. Debbah, and D. T. M. Slock, "Large System Analysis of Linear Precoding in MISO Broadcast Channels with Limited Feedback," *IEEE Trans. Inf. Theory*, vol. 58, no. 7, pp. 4509–4537, July 2012.
- [13] R. Muharar and J. Evans, "Downlink beamforming with transmit-side channel correlation: A large system analysis," in *Proc. IEEE Int. Conf. Commun. (ICC)*, 2011.
- [14] R. Couillet and M. Debbah, *Random matrix methods for wireless communications*, Cambridge University Press, New York, NY, USA, first edition, 2011.
- [15] E. Björnson, M. Bengtsson, and B. Ottersten, "Pareto characterization of the multicell MIMO performance region with simple receivers," *IEEE Trans. Signal Process.*, vol. 60, no. 8, pp. 4464–4469, Aug. 2012.
- [16] C. B. Peel, B. M. Hochwald, and A. L. Swindlehurst, "A vector-perturbation technique for near-capacity multiantenna multiuser communication, Part I: Channel inversion and regularization," *IEEE Trans. Commun.*, vol. 53, no. 1, pp. 195–202, Jan. 2005.
- [17] T.K.Y. Lo, "Maximum ratio transmission," *IEEE Trans. Commun.*, vol. 47, no. 10, pp. 1458–1461, Oct. 1999.
- [18] S. Moshavi, E.G. Kanterakis, and D.L. Schilling, "Multistage linear receivers for DS-CDMA systems," *Int. J. Wireless Information Networks*, vol. 3, no. 1, pp. 1–17, Jan. 1996.
- [19] M.L. Honig and W. Xiao, "Performance of reduced-rank linear interference suppression," *IEEE Trans. Inf. Theory*, vol. 47, no. 5, pp. 1928–1946, July 2001.
- [20] G. Sessler and F. Jondral, "Low complexity polynomial expansion multiuser detector for CDMA systems," *IEEE Trans. Veh. Technol.*, vol. 54, no. 4, pp. 1379–1391, July 2005.
- [21] J. Hoydis and M. Debbah and M. Kobayashi, "Asymptotic Moments for Interference Mitigation in Correlated Fading Channels," in *Proc. Int. Symp. Inf. Theory (ISIT)*, 2011.
- [22] N. Shariati, E. Björnson, M. Bengtsson, and M. Debbah, "Low-complexity channel estimation in large-scale MIMO using polynomial expansion," in *Proc. IEEE Int. Symp. Personal, Indoor and Mobile Radio Commun. (PIMRC)*, 2013.
- [23] S. Zarei, W. Gerstacker, R. R. Müller, and R. Schober, "Low-Complexity Linear Precoding for Downlink Large-Scale MIMO Systems," in *Proc. IEEE Int. Symp. Personal, Indoor and Mobile Radio Commun. (PIMRC)*, 2013.
- [24] A. Kammoun, A. Müller, E. Björnson, and M. Debbah, "Linear precoding based on truncated polynomial expansion—Part II: large-scale multi-cell systems," *IEEE J. Sel. Topics Signal Process.*, Sept. 2013, Submitted, arXiv:1310.1799.
- [25] J. Choi, D.J. Love, and P. Bidigare, "Downlink training techniques for FDD massive MIMO systems: Open-loop and closed-loop training with memory," *IEEE J. Sel. Topics Signal Process.*, Sept. 2013, Submitted, arXiv:1309.7712.
- [26] C. Wang and R.D. Murch, "Adaptive downlink multi-user MIMO wireless systems for correlated channels with imperfect CSI," *IEEE Trans. Wireless Commun.*, vol. 5, no. 9, pp. 2435–2436, Sept. 2006.
- [27] B. Nosrat-Makouei, J.G. Andrews, and R.W. Heath, "MIMO interference alignment over correlated channels with imperfect CSI," *IEEE Trans. Signal Process.*, vol. 59, no. 6, pp. 2783–2794, Jun. 2011.
- [28] E. Björnson and E. Jorswieck, "Optimal resource allocation in coordinated multi-cell systems," *Foundations and Trends in Communications and Information Theory*, vol. 9, no. 2-3, pp. 113–381, 2013.
- [29] M. Joham, W. Utschick, and J.A. Nossek, "Linear transmit processing in MIMO communications systems," *IEEE Trans. Signal Process.*, vol. 53, no. 8, pp. 2700–2712, Aug. 2005.
- [30] M. Sadek, A. Tarighat, and A.H. Sayed, "A leakage-based precoding scheme for downlink multi-user MIMO channels," *IEEE Trans. Wireless Commun.*, vol. 6, no. 5, pp. 1711–1721, May 2007.
- [31] R. Stridh, M. Bengtsson, and B. Ottersten, "System evaluation of optimal downlink beamforming with congestion control in wireless communication," *IEEE Trans. Wireless Commun.*, vol. 5, no. 4, pp. 743–751, Apr. 2006.
- [32] E. Björnson, R. Zakhour, D. Gesbert, and B. Ottersten, "Cooperative multicell precoding: Rate region characterization and distributed strategies with instantaneous and statistical CSI," *IEEE Trans. Signal Process.*, vol. 58, no. 8, pp. 4298–4310, Aug. 2010.
- [33] C. Shepard, H. Yu, N. Anand, L.E. Li, T. Marzetta, R. Yang, and L. Zhong, "Argos: Practical many-antenna base stations," in *Proc. ACM MobiCom*, 2012.
- [34] S. Boyd and L. Vandenberghe, "Numerical linear algebra background," <http://www.ee.ucla.edu/ee236b/lectures/num-lin-alg.pdf>.
- [35] V. Strassen, "Gaussian elimination is not optimal," *Numer. Math.*, vol. 13, pp. 354–356, 1969.
- [36] V.V. Williams, "Multiplying matrices faster than Coppersmith-Winograd," in *Proc. Symp. Theory Comp. (STOC)*, 2012, pp. 887–898.
- [37] E. Dahlman, S. Parkvall, and J. Sköld, *4G: LTE/LTE-Advanced for Mobile Broadband: LTE/LTE-Advanced for Mobile Broadband*, Academic Press, 2011.
- [38] C. Dick, F. Harris, M. Pajic, and D. Vuletic, "Implementing a real-time beamformer on an FPGA platform," in *Xcell J.*, 2007.
- [39] S.L. Loyka, "Channel capacity of MIMO architecture using the exponential correlation matrix," *IEEE Commun. Lett.*, vol. 5, no. 9, pp. 369–371, 2001.
- [40] G.H. Golub and C.F. Van Loan, *Matrix Computations*, The Johns Hopkins University Press, 1996.
- [41] W. Rudin, *Real and complex analysis*, McGraw-Hill Series in Higher Mathematics, third edition, May 1986.
- [42] S. Boyd and L. Vandenberghe, *Convex Optimization*, Cambridge University Press, New York, 2004.